

On the importance of phenology-water interactions in the evaporative process of a semi-arid woodland: Could it be why satellite-based evaporation estimates in the Miombo woodlands differ?

5 *Henry M. Zimba^{1,2}, Miriam Coenders-Gerrits¹, Kawawa E. Banda³, Petra Hulsman⁴, Nick van de Giesen¹, Imasiku A. Nyambe³, Hubert. H. G. Savenije¹.

¹ Water Resources Section, Faculty of Civil Engineering and Geosciences, Delft University of Technology, Stevinweg 1, 2628 CN Delft, The Netherlands.

² Department of Agriculture, Ministry of Agriculture, P.O. Box 50595, Mulungushi House, Independence Avenue, Lusaka, Zambia.

³ Integrated Water Resources Management Centre, Department of Geology, School of Mines, University of Zambia, Great East Road Campus, Lusaka, Zambia.

⁴ Ghent University, Hydro-Climate Extremes Lab (H-CEL), Coupure links 653, 9000 Ghent, Belgium

15 *Corresponding author: a.m.j.coenders@tudelft.nl

Abstract

20 The miombo woodland is the largest dry woodland formation in sub-Saharan Africa with a spatial extent approximated between 2.7 – 3.6 million km². In comparison to other global ecosystems the miombo woodland exhibits unique ecohydrological properties such as increase in the leaf area index (LAI) in the dry season. However, due to limited flux observations in the miombo region, there is scarcity of information on the effect of these properties on evaporation of the miombo woodland. Better understanding of evaporation of the miombo is required for accurate hydrological and climate modelling of this region. The only regional evaporation estimates available are from satellite-based products. However, due to the scarcity of information, there is doubt about their accuracy. Therefore, in this study trends and magnitudes of six satellite-based evaporation estimates (FLEXI-Topo, GLEAM, MOD16, SSEBop, TerraClimate and WaPOR) are compared over the different seasons in the miombo woodland of the Luangwa Basin, a representative river basin in southern Africa. In this comparison we check if the trends and magnitudes of the satellite-based evaporation estimates align with the documented phenology-water interactions of the miombo woodland. In the absence of basin scale field observations, actual evaporation estimates based on the multi-annual water balance (E_{wb}) are used for comparison.

35 Results show that satellite-based evaporation estimates differ substantially from each other within the different seasons, i.e., the cool-dry season, warm dry season and warm-pre-rainy season. The latter is a characteristic season when the miombo species undergo substantial changes in the canopy phenology, whereby ~~leaf fall~~leaf-fall and ~~leaf flush~~leaf-flush occur at the same time, and there is access to deeper moisture stocks to support ~~leaf flush~~leaf-flush in preparation of the rainy season. During the ~~warm dry season~~season, the ~~satellite-based evaporation estimates products~~ differ most from each other, while the best agreement is reached during the ~~periods with~~rainy season ~~with~~ high temperature, ~~high soil moisture~~, high leaf chlorophyll content and highest LAI (i.e., rainy season). Compared to the basin-scale actual evaporation, all six satellite-based evaporation estimates appear to underestimate evaporation. Overall, it appears that inadequate

understanding and inaccurate representation of the phenology-water interactions of the miombo species are the cause of these discrepancies. Based on this study, field-based observations of the evaporation during the different seasons are required to enhance satellite-based evaporation estimates in the miombo woodlands.

1 Introduction

Vegetation phenology refers to the periodic biological life cycle events of plants, such as ~~leaf flush~~leaf-flushing, senescence and corresponding temporal changes in vegetation canopy cover (Stöckli *et al.*, 2011; Cleland *et al.*, 2007). Plant phenology and climate are highly correlated (Pereira *et al.*, 2022; Niu *et al.*, 2013; Cleland *et al.*, 2007). Plants respond to triggers, such as temperature, hydrology and day light, by initiating among others: ~~leaf fall~~leaf-fall, ~~leaf flush~~leaf-flush, budburst, flowering and variation in photosynthetic activity (Pereira *et al.*, 2022; Niu *et al.*, 2013; Cleland *et al.*, 2007). Phenological responses are species-dependent and are controlled by adapted physiological properties (i.e., Lu *et al.*, 2006). Plant phenology controls the access to critical soil resources such as nutrients and water (Nord and Lynch, 2009).—Moreover, phenological response influences plant canopy cover and affects plant-water interactions. Variations in canopy leaf display, i.e., due to ~~leaf fall~~leaf-fall and ~~leaf flush~~leaf-flush, influences how much radiation is intercepted by plants (Shahidan, Salleh, and Mustafa, 2007). Intercepted radiation influences canopy conductance. In water limited conditions, at both individual species and woodland scales, ~~leaf fall~~leaf-fall reduces canopy radiation interception while ~~leaf flush~~leaf-flush and the consequent increase in canopy cover increases canopy radiation interception leading to increased transpiration (Snyder and Spano, 2013), controlled by moisture availability, whether in the vegetation itself or in the root zone. Plant canopy cover and its interactions with atmospheric carbon dioxide influences transpiration. Ultimately, plant phenological response to changes in the triggers influences transpiration and actual evaporation of the woodland (i.e., Marchesini *et al.*, 2015). _____ Evaporation of woodland surfaces accounts for a significant portion of the water cycle over the terrestrial landmass (Sheil, 2018; Van Der Ent *et al.*, 2014; Gerrits, 2010; Van Der Ent *et al.*, 2010). Miralles *et al.* (2020) defined evaporation as “the phenomenon by which a substance is converted from its liquid into its vapour phase, independently of where it lies in nature”. In this study we adopt the term evaporation for all forms of terrestrial evaporation, including transpiration by leaves, evaporation from intercepted rainfall by vegetation and woodland floor, soil evaporation, and evaporation from stagnant open water and pools (Savenije, 2004). Understanding the characteristics of evaporation, such as interception and transpiration, in various woodland ecosystems is key to monitoring the climate impact on woodland ecosystems and for hydrological modelling and the management of water resources at various scales (Kleine *et al.*, 2021; Bonnesoeur *et al.*, 2019; Roberts, (undated)). Knowledge of the woodland phenology interactions with climate variables and seasonal environmental regimes is key to this understanding (i.e., Zhao *et al.*, 2013). Environmental variables such as precipitation and temperature influences plant phenology differently across the diverse ecosystems globally (Forrest *et al.*, 2010; Forrest & Miller-Rushing, 2010; Kramer *et al.*, 2000). Additionally, Tian *et al.* (2018) showed that, at the ecosystem scale, plants have adapted to local climatic (such as precipitation, temperature, and radiation) and abiotic (such as soil type and soil water supply) conditions. The findings by Tian *et al.* (2018) are “evidence of global differences in the interaction between plant water storage and leaf phenology”. Although this study referred to

within-plant storage of moisture it may be as relevant to root zone storage or access to groundwater. Therefore, understanding the plant phenology-water interactions at local and regional scales and appropriately incorporating these aspects in hydrological and climate modelling is likely to improve accuracy of the simulations (i.e., Forster *et al.*, 2022).

The miombo woodlands is the largest dry woodland formation in sub-Saharan Africa with a spatial extent approximated between 2.7 – 3.6 million km², covering about 10% of the continent (Ryan *et al.*, 2016; Frost, 1996; White, 1983). Despite their significance for biodiversity (Mittermeier *et al.*, 2003; White, 1983), carbon sink (Pelletier *et al.*, 2018) and the food, energy and water nexus (Beilfuss, 2012; Campbell *et al.*, 1996; Frost, 1996), little attention has been paid to its hydrological functioning. The uniqueness of its plant-water interactions has been highlighted (Tian *et al.*, 2018; Guan *et al.*, 2014; White, 1983) and has been particularly demonstrated by Tian *et al.* (2018), Vinya *et al.*, (2018), Fuller (1999), Frost (1996) and White (1983). Of particular importance is its control of leaf phenology (i.e., Vinya *et al.*, 2018), ~~simultaneous co-occurring of leaf-fall|leaf-fall~~ (leaf shedding) and ~~leaf-flush|leaf-flush~~ (i.e., Fuller, 1999), and deep rooting, which allows miombo species to access deep soil moisture, including groundwater, to buffer for dry season water limitations (Tian *et al.*, 2018; Guan *et al.*, 2014; Savory, 1963). Most remarkably, new ~~leaf-flush|leaf-flush~~ occurs before the commencement of seasonal rainfall (Chidumayo, 1994; Fuller and Prince, 1996). Young flushed leaves in the dry season have high water content of up to 66% which declines to about 51% as the leaves harden, until they are shed off in the next season (Ernst and Walker, 1973). The miombo woodland is heterogeneous with diverse plant species whose phenological response to stimuli is species-dependent (Chidumayo, 2001; Fuller, 1999; Frost, 1996). For instance, ~~leaf-fall|leaf-fall~~, ~~leaf-flush|leaf-flush~~ and leaf colour change are triggered at different times for each species. This means that the miombo woodland is unlike other woodlands where ~~leaf-fall|leaf-fall~~ and ~~leaf-flush|leaf-flush~~ occur in different seasons. In the Miombo, co-occurring of ~~simultaneous leaf-fall|leaf-fall~~ and ~~leaf-flush|leaf-flush~~ results in a woodland canopy that is variable in terms of canopy closure and greenness especially during the dry season. As a result, it has varied canopy closure ranging from 2 to about 70 percent depending on the miombo woodland strata and local environmental conditions such as rainfall, soil type, soil moisture, species composition and temperature (Chidumayo, 2001; Fuller, 1999; Frost, 1996). For the wet miombo woodland with a canopy closure of about 70 percent, at any given time, there is a relatively large woodland canopy surface for radiation interception. The deep rooting in most miombo species (Savory, 1963) provides access to deep soil moisture resources (Fan *et al.*, 2017; Kleidon and Heimann, 1998). As a result, the canopy provides an evaporative surface that, in combination with other environmental variables, possibly facilitates continued transpiration even during the driest periods (i.e., Li *et al.*, 2021). Most miombo species are broad leaved with capacity for radiation interception (Fuller, 1999) and rainfall interception of up to 20% in wet miombo woodland (Alexandre, 1977). It appears that in the miombo woodland soil moisture increases with depth (Chidumayo, 1994; Jeffers and Boaler, 1996; Savory, 1963). These typical phenological and physiological attributes are of particular importance for evaporative processes (Forster *et al.*, 2022; Snyder *et al.*, 2013; Schwartz, 2013).

Regardless of the uniqueness and importance of the miombo woodland, there exists scant, if any, information on its evaporation dynamics. Most of studies in the miombo woodland concentrated on the characterisation of woodland plant species, its role as a carbon sink and the social-economic relevance of the ecosystem. There is ample information on the phenology of plant species (e.g.: Chidumayo *et al.*, 2010; Chidumayo, 2001; Fuller, 1999; Chidumayo and Frost, 1996), but there have been very limited attempts to characterise evaporation of the ecosystem,

135 especially during the dry season. The only point-based field observations of evaporation of the wet
miombo woodland by Zimba *et al.* (2013) are not sufficient to make any definitive conclusions
about the evaporative dynamics of this vast ecosystem.

140 In the absence of spatially distributed field observations, satellite-based evaporation
estimates are valuable alternatives, though they come with their own limitations (Zhang *et al.*,
2016). It is well-realised that evaporation depends on land cover (Han *et al.*, 2019; Liu & Hu,
2019; Wang *et al.*, 2012), but, because of the differences in algorithms, process and inputs,
145 satellite-based evaporation estimates differ for the same land surface (Zhang *et al.*, 2016; Cheng
et al., 2014). Currently, satellite-based evaporation estimates at various scales are available (e.g.:
Global land evaporation Amsterdam model (GLEAM) (Martens *et al.*, 2017; Miralles *et al.*, 2011);
Moderate-resolution imaging spectrometer (MODIS) MOD16) (Running *et al.*, 2019; Mu *et al.*,
2011; Mu *et al.*, 2007); Operational simplified surface energy balance (SSEBop) (Senay *et al.*,
145 2013); and Water productivity through open access of remotely sensed derived data (WaPOR)
(FAO, 2018)). Classification of the various satellite-based evaporation estimates have been
extensively discussed by Zhang *et al.* (2016), Jiménez *et al.* (2011) and Jiménez, Prigent & Aires
(2009). These satellite-based evaporation estimates have mainly been designed for agricultural
crops (i.e., Biggs *et al.*, 2015; Zhang *et al.*, 2016). However, natural woodlands have different
150 phenology-water interactions and evaporation characteristics (Wang-Erlandsson *et al.*, 2016;
Snyder and Spano, 2013; Schwartz, 2013). There is currently no publication in the public domain
showing how various satellite-based evaporation estimates compare in the miombo woodland,
especially with a focus on the unique interactions between phenology and hydrology in miombo
species across different phenophases and seasons. Yet, the use of satellite-based evaporation
155 estimates in hydrological modelling, climate modelling and the management of water resources,
globally and in Africa, is increasing (i.e., García *et al.*, 2016; Zhang *et al.*, 2016; Makapela, 2015).
However, because of the absence or scarce field observations and extremely limited validation, it
is impossible to know which satellite-based evaporation estimates are close to the actual conditions
of the miombo woodland. If any, the choice for a satellite-based evaporation product is based on
160 validation results in non-miombo woodlands or at a scale (i.e., Weerasinghe *et al.*, 2020) that
includes other woodland types. Obviously, an evaporation estimation approach that performs well
in energy limited conditions or homogeneous woodlands (i.e., Bogawski and Bednorz, 2014)
cannot be assumed to have the same performance in a warm, water limiting and heterogeneous
woodland such as the miombo. Although, Weerasinghe *et al.* (2020) compared satellite-based
165 evaporation estimates in the Zambezi Basin, whose vegetation cover, among many others,
comprises the miombo woodland, the focus of their study was not on the miombo woodland.
Furthermore, Weerasinghe *et al.* (2020) did not attempt to link the differences in the satellite-based
evaporation estimates to the phenology of the miombo woodland. The results they observed at the
Zambezi Basin scale might be different at sub-basin level such as the Luangwa Basin.

170 This study addresses the performance of satellite-based evaporation estimates during
different phenophases of the miombo woodland with a focus on the Luangwa sub-basin of the
Zambezi, one of the largest river basins in the miombo ecosystem. The Luangwa basin contains
both dry (i.e., southern miombo woodlands) and wet (i.e., central Zambezian miombo woodlands)
miombo. The central Zambezian miombo woodland is the largest of the four miombo woodland
175 sub-groups, the other three being the Angolan miombo woodland, eastern miombo woodland, and
the southern miombo woodland (Frost, 1996; White, 1983). The Luangwa Basin is largely covered
by miombo woodland with the mopane woodland occupying a much smaller area of the basin

(Frost, 1996; White, 1983). These attributes suggest a catchment that provides a fair representation of miombo woodlands and an appropriate site for studying its evaporation characteristics.

Hence, the aim of this study is two-fold:

- (i) Compare the temporal trends and magnitudes of six freely available satellite-based evaporation products across different phenophases of the miombo woodland.
- (ii) Compare satellite-based evaporation estimates to the water balance-based actual evaporation estimates for the Luangwa Basin.

2 Materials and Methods

2.1 Study site

The location and extent of the miombo woodland in Africa is presented in Fig. 1(a) (Ryan *et al.*, 2016; White, 1983). The Luangwa (Fig. 1b) is a sub-basin of the Zambezi Basin in sub-Saharan Africa in Zambia with spatial extent of about 159,000 km² (Beilfuss, 2012; World Bank, 2010). Based on the miombo woodland delineation by White (1983) and Ryan *et al.* (2016) as given in Fig.1 (c) about 75 percent of the total Luangwa Basin land-mass is covered by the miombo woodland, both dry and wet miombo.

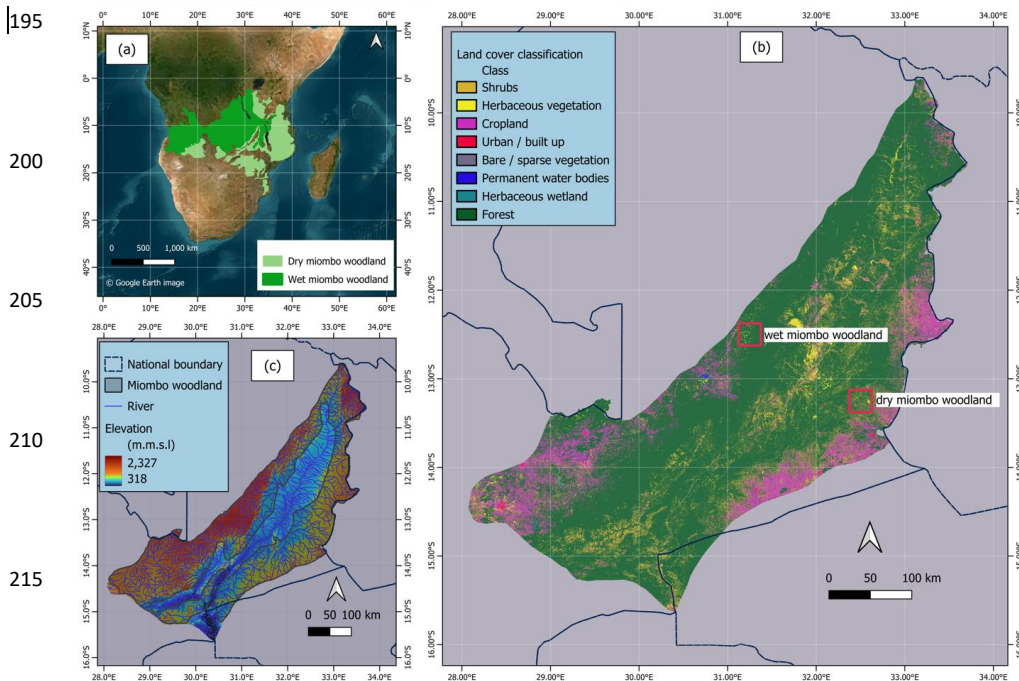


Figure 1: (a) Spatial extent of the miombo woodland in Africa and the location of the Luangwa Basin in Zambia. (b) Spatial distribution of elevation ASTER digital elevation model (DEM) and the extent of the miombo woodland in the Luangwa Basin. (c) Land cover characterisation of the Luangwa Basin based on the Copernicus land cover classification.

225 Additionally, statistics from the 2019 Copernicus land cover classification (Fig. A1 in the
supplementary data), indicates that 77 % of the total basin area is woodland (dense and open
woodland) which is largely miombo woodland with a smaller component of mopane woodland in
the middle area of the basin (Buchhorn *et al.*, 2020; Martins *et al.*, 2020). Elevation (Fig. 1b)
230 ranges between 329 – 2210 m with the central part generally a valley. The miombo woodland,
both dry and wet miombo, is generally in the upland (Fig.1b). The Luangwa River, 770 km long,
drains the basin and is scarcely gauged (Beilfuss, 2012). This has resulted in a paucity of data on
various hydrological aspects such as rainfall and discharge. The climate is characterised by a well-
delineated wet season, from October to April, and a dry season, from May to October. Furthermore,
the dry season is split into the cool-dry (May to August) and hot dry (August to October) seasons.
235 The movement of the inter-tropical convergence zone (ITCZ) over Zambia between October and
April dominates the rainfall activity in the basin. The basin has a mean annual precipitation of
about 970 mm yr⁻¹, potential evaporation of about 1560 mm yr⁻¹, and river runoff reaches about
100 mm yr⁻¹ (Beilfuss, 2012; World Bank, 2010). The key character of the miombo woodland
species is that it sheds off old leaves and acquires new ones during the period May to October
240 during the dry season. Depending on the amount of rainfall received in the preceding rain season
the ~~leaf fall~~leaf-fall and ~~leaf flush~~leaf-flush processes may start early (i.e., in case of low rainfall
received) or late (in case of high rainfall received) and may continue up to November (i.e., in the
case of high rainfall received) (Frost,1996).

245 2.2 Study approach

The study sought to find out the extent to which satellite-based evaporation estimates agree
with each other during the different canopy phenophases of the miombo woodland. Point scale
observations in the wet miombo woodland (Zimba *et al.*, 2023) showed that satellite-based
evaporation estimates underestimated actual evaporation of the wet miombo woodland during the
250 dry season and early rainy season in the Luangwa Basin. However, the Luangwa Basin has a
heterogenous land cover which includes mopane woodland and grasslands. The question was
whether the heterogeneity in the land cover of the Luangwa Basin would result in satellite-based
evaporation estimates performing contrary to the point-scale observations at a wet miombo
woodland site when compared to the water balance-based evaporation estimates at basin scale.

255 For this study, a 12-year period, 2009–2020, was used because satellite-based evaporation
estimates were available for free for this period. The period also had cycles of low and high annual
rainfall allowing to analyse performance under changing monthly and annual conditions. The
following sections elaborate the methods used in this study.

260 2.2.1 Phenophases of the miombo woodland and assessment of phenological conditions

To categorise the phenophases two approaches were used: satellite-based classification and
climate and soil moisture-based classifications.

Satellite-based classification of phenophases has been based on the National Aeronautics
and Space Administration (NASA) Collection 6 MODIS Land Cover Dynamics (MCD12Q2)
265 Product accessed from the <https://modis.ornl.gov/globalsubset/>, last access: 20 February, 2023
(Gray *et al.*, 2019; Friedl *et al.*, 2019; Zhang *et al.*, 2003). The MCD12Q2 uses the changes in
canopy greenness to characterise the canopy phenophases (Friedl *et al.*, 2019; Gray *et al.*, 2019).
For the miombo woodland in the Luangwa Basin eight phenophases were identified using the
satellite-based data MCD12Q2 (Fig. 2). The satellite-based phenophases include: green-up, mid-

270 green up, maturity, peak, senescence, green-down, and mid-green down and dormant. For easy of
 analysis the phenophases were merged into four groups based on dominant activity in each
 phenophase (Fig. 2). To compliment the MCD12Q2 classification the MODIS-based leaf area
 index (LAI) obtained from <https://modis.ornl.gov/globalsubset/> and <https://app.climateengine.org/ClimateEngine>, last access: 20
 275 February, 2023) (Myneni, Knyazikhin & Park, 2021; ORNL DAAC, 2018; Myneni & Park, 2015)
 and the normalised difference vegetation index (NDVI) (ORNL DAAC, 2018; Vermote and Wolfe,
 2015) were used.

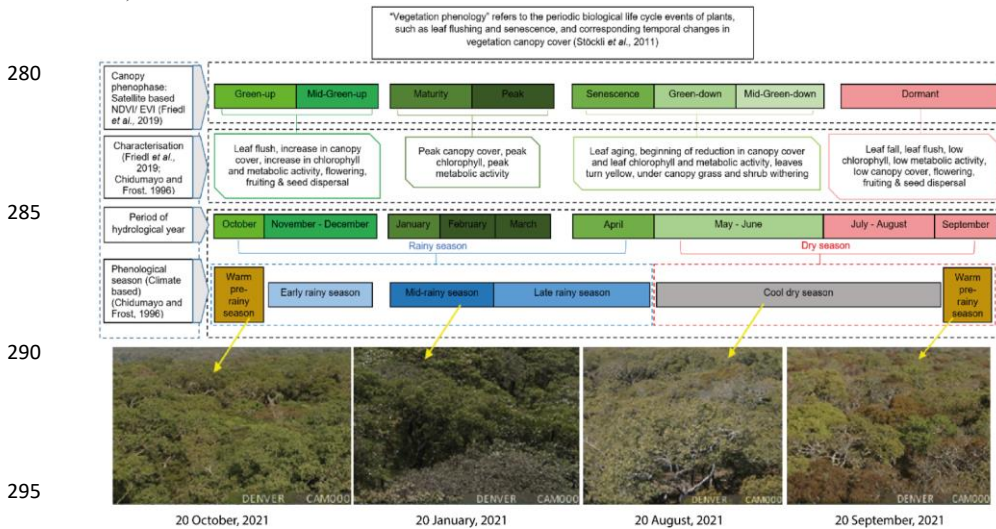


Figure 2: Characterisation of canopy phenophases of the miombo woodland in relation to seasonality for the Luangwa Basin. Photographs show the changes in the canopy cover on selected days across different phenophases of a wet miombo woodland for the year 2021.

300 The satellite-based LAI and NDVI have been used before as proxies to observe
 phenological conditions such as the canopy biomass formation, changes in the canopy closure (i.e.,
 through leaf-fall and leaf-flush) and changes in canopy chlorophyll conditions (i.e., Guan *et al.*,
 2014; Santin-Janin *et al.*, 2009; Chidumayo, 2001; Fuller, 1999). For the LAI the NASA's
 305 MCD15A3H product (Myneni, Knyazikhin & Park, 2021; ORNL DAAC, 2018; Myneni & Park,
 2015) with a four-day temporal resolution and 500 m spatial resolution has been used. The MODIS
 MOD09GQ.006 (Vermote and Wolfe, 2015) surface reflectance bands 1,5 and 6 have been used
 to estimate the NDVI at daily temporal resolution and 250 m spatial resolution using the band ratio
 method. The daily NDVI values were then averaged into four-day values to obtain the same
 310 temporal resolution as the LAI.

For the climate and soil moisture-based classification Chidumayo and Frost (1996)
 observed five phenological seasons: warm pre-rainy season, early rainy season, mid-rainy season,
 late rainy season and the cool dry season (Fig. 2). For easy of analysis, the above three rainy season
 phenophases were merged into one rainy season phenophase. Therefore, three climate and soil
 315 moisture-based phenophases were established; warm pre-rainy season, rainy season and the cool

dry season. Within these phenological seasons the phenology of miombo species transitions through various stages i.e., from leaf-fall/leaf-flush, growth of stems, flowering to mortality of seed (Chidumayo and Frost, 1996).

To compliment the observations, photographs from a digital camera (Denver WCT-8010) installed on the flux tower at a wet miombo woodland site in Mpika (Zimba *et al.*, 2023) were used to observe the changes in the canopy phenology of the miombo woodland across different phenophases from January to December in the year 2021. In addition, the fish-eye (LIEQI LQ-001) was used to obtain under-canopy images. The images of from under-the canopy helped to observe the changes and differences in canopy leaf display (i.e., leaf-fall, leaf-flush and leaf colour changes) among miombo species.

2.2.2 Delineation of the miombo woodland areas used in this study

The comparison of satellite-based evaporation estimates was performed at two levels: pixel using a grid at a level at known dry miombo woodland and wet miombo woodland locations, and at the entire miombo woodland scale in the Luangwa Basin (Figs. 1 and 3).

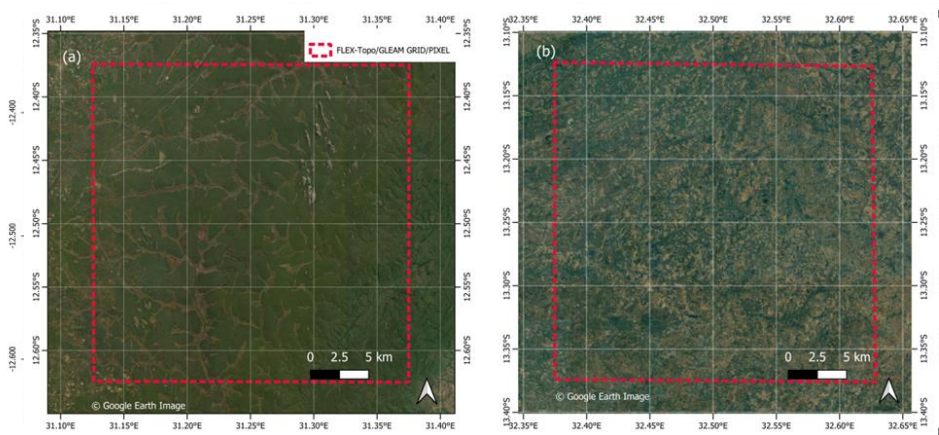


Figure 3: The wet miombo woodland (a) and dry miombo woodland (b) locations used for comparison of satellite-based evaporation estimates at FLEX-Topo and GLEAM spatial resolution (approximately 27.7 km by 27.7 km). The dotted red line is the actual location of the FLEX-Topo and GLEAM pixels.

Firstly, a pixel-based comparison based on the 27.7km by 27.7km grid was performed by using known undisturbed wet miombo woodland and dry miombo woodland locations (Figs. 1 and 3). The pixel-grid was based comparison based-used on the satellite-based evaporation estimates (i.e., FLEX-Topo and GLEAM) with the largest spatial resolutions - actual location of FLEX-Topo and GLEAM pixels with original spatial resolutions - (approximately 27.7 km by 27.7 km) (Fig. 3 and Table 1). For MOD16, SSEBop, TerraClimate and WaPOR, the mean of actual evaporation estimates in in all the pixels within the dotted red square (Fig. 3) were used. The focus on a known wet miombo woodland enabled comparison of the field observations of the changes in canopy

cover using digital camera images to the satellite-based LAI and NDVI for the year 2021. ~~The pixel based comparison used actual location of FLEX-Topo and GLEAM pixels with original spatial resolutions (approximately 27.7 by 27.7 km) (Fig. 3). For MOD16, SSEBop, TerraClimate and WaPOR, the mean of actual evaporation estimates in all the pixels within the dotted red square (Fig. 3) were used.~~ See Section 2.2.3 and Table 1 for satellite-based evaporation estimates used in this study.

Secondly, the typical miombo woodland regions as categorised by White (1983) and Ryan *et al.* (2016) (see Fig. 1 a,b) were used to delineate the area covered by the miombo woodland in the Luangwa Basin. The delineated miombo woodland in the Luangwa Basin excluded the mopane woodland, mixed woodland as well as the water bodies. This delineation (as shown in Fig. 1) ensured that only the areas classified as typical miombo woodland (Ryan *et al.*, 2016; White, 1983) were considered in the analysis.

2.2.3 Satellite-based products used in the study

The six satellite-based evaporation estimates consisted of: 1) FLEX-Topo (Hulsman *et al.*, 2021; Hulsman *et al.*, 2020; Savenije, 2010); 2) Thornthwaite-Mather climatic water balance model (TerraClimate) (Abatzoglou *et al.*, 2018); 3) Global land evaporation Amsterdam model (GLEAM) (Martens *et al.*, 2017; Miralles *et al.*, 2011); 4) Moderate-resolution imaging spectrometer (MODIS) MOD16 (Running *et al.*, 2019; Mu *et al.*, 2011; Mu *et al.*, 2007); 5) Operational simplified surface energy balance (SSEBop) (Senay *et al.*, 2013) and 6) Water productivity through open access of remotely sensed derived data (WaPOR) (FAO, 2018). These satellite-based evaporation estimates were selected purely because they are free of charge and easily accessible from various platforms and have an archive of historical data with the temporal and spatial resolutions suitable for use in this study. Except for FLEX-Topo and GLEAM (with spatial resolution of 27.7 km), these satellite-based evaporation estimates have relatively fine spatial resolution (i.e., 500 m, 1000 m, 4000 m and 250 m for MOD16, SSEBop, TerraClimate and WaPOR respectively) and temporal resolution (daily, 8-day, 10-day and monthly respectively), which attributes were suitable for this study. The original spatial resolutions were used because these satellite-based evaporation estimates are normally used as is, in their original resolutions. Resampling the different spatial resolutions of the satellite-based evaporation estimates to a single (uniform) spatial resolution was thought to be problematic as it would have introduced unknown and unquantifiable errors, regardless the extent resampled. For detailed explanations on the model structure, processes and inputs for the satellite-based evaporation estimates used in this study the reader is advised to refer to the cited literature above and in Table 1.

Other satellite-based products used in this study include the ASTER digital elevation model (DEM), MODIS-based LAI and NDVI, Copernicus land cover map, net radiation, precipitation, runoff, soil moisture and relative humidity. For detailed information (i.e., structure, processes and inputs) on the other satellite-based products used in this study the reader is advised to refer to the cited literature in Table 1.

2.2.4 Actual evaporation derived from the water balance

In cases where spatially distributed field measurements are not available the water balance approach, using spatially distributed satellite-data, is a practical approach (i.e., Weerasinghe *et al.*, 2020; Liu *et al.*, 2016). In this study the general annual water balance was used to test the performance of the satellite-based evaporation estimates at basin level.

Table 1. Characteristics of products used in the study

| Variable | Product name | Time Period | Spatial coverage/Location | Temporal resolution | Spatial resolution | Reference | Source of data |
|------------------------|--------------------------|-------------|---------------------------|---------------------|--------------------|--|---|
| Precipitation | CFSR v2 | 2009 - 2020 | Global | Daily | 19.2 km | (Saha <i>et al.</i> , 2014; Saha <i>et al.</i> , 2010) | Climate Engine portal |
| | CHRRS | 2009 - 2020 | Global | Daily | 4.8 km | (Funk <i>et al.</i> , 2015) | https://app.climateengine.com/ClimateEngine |
| | ERA5 | 2009 - 2020 | Global | Daily | 24 | (Hersbach <i>et al.</i> , 2017) | Climate Engine portal |
| Air temperature (mean) | TerraClimate | 2009 - 2020 | Global | Monthly | 4 km | (Abatzoglou <i>et al.</i> , 2018) | Climate Engine portal |
| | CFSR v2 | 2009 - 2020 | Global | Daily | 19.2 km | (Saha <i>et al.</i> , 2014; Saha <i>et al.</i> , 2010) | Climate Engine portal |
| LAI | MODIS MCD15A3H v6 | 2021 | Global | 4-Day | 0.5 km | (Myeni, Kinyazhina & Park, 2015) | Climate Engine portal |
| NDVI | MODIS MOD09GA v6 | 2021 | Global | Daily | 0.5 km | (Vermote & Wolfe, 2015) | Climate Engine portal |
| | Observations | 1960-1992 | 159,000 km ² | Daily | N/A | | WARMA, Zambia |
| Rumoff | TerraClimate | 1960 - 2020 | Global | Monthly | 4 km | (Abatzoglou <i>et al.</i> , 2018) | Climate Engine portal |
| Net radiation | CFSR v2 | 2009-2020 | Global | Daily | 19.2 km | (Saha <i>et al.</i> , 2014; Saha <i>et al.</i> , 2010) | Climate Engine portal |
| Soil moisture (25 cm) | CFSR v2 | 2009 -2020 | Global | Daily | 19.2 km | (Saha <i>et al.</i> , 2014; Saha <i>et al.</i> , 2010) | Climate Engine portal |
| Relative humidity | CFSR v2 | 2009 - 2020 | Global | Daily | 19.2 km | (Saha <i>et al.</i> , 2014; Saha <i>et al.</i> , 2010) | Climate Engine portal |
| Elevation | ASTER GDEM v3 | N/A | Global | N/A | 30m | (Abrams and Crispin, 2019) | NASA Giovis portal |
| Land cover map | Copernicus CGLS-LC100 v3 | 2019 | Global | Annual | 100m | (Buchhorn <i>et al.</i> , 2020) | Google Earth Engine |
| Actual evaporation | FLEX-Topo | 2009 - 2020 | Catchment | Daily | 27.7 km | (Huisman <i>et al.</i> , 2021; Huisman <i>et al.</i> , 2020; Savicije, 2010) | ZAMSECUR Project – Delft Technical University |
| | GLEAM (v3.2a) | 2009 -2020 | Global | Daily | 27.7 km | (Martens <i>et al.</i> , 2017; Miralles <i>et al.</i> , 2011) | GLEAM FTP server |
| | MOD16v2 | 2009 -2020 | Global | 8-Day | 0.5 km | (Running <i>et al.</i> , 2019; Mu <i>et al.</i> , 2011) | Climate Engine portal; Global subsets tool: MODIS VIIRS Land Products |
| TerraClimate | SSERBP | 2009 -2020 | Global | Monthly | 1 km | (Senay <i>et al.</i> , 2013). | Climate engine portal |
| | TerraClimate | 2009 -2020 | Global | Monthly | 4 km | (Abatzoglou <i>et al.</i> , 2018) | Climate engine portal |
| WaPOR v2 (ETLook) | WaPOR v2 (ETLook) | 2009 -2020 | Continental | 10-Day | 0.25 km | (FAO, 2018) | WaPOR Portal |

405

410

415

420

425

430

435

440

445

450

455

The basin average annual water balance-based evaporation ($E_{a(wb)}$) is estimated using Eq. (1) where long-term over-year storage change is disregarded.

460

$$E_{a(wb)} = P - Q \quad (1)$$

where, P is the annual average catchment precipitation in mm year^{-1} and Q is annual average discharge in mm year^{-1} . The precipitation and discharge information for the water balance approach were selected and used as explained below.

465

Ensemble satellite precipitation

The challenge posed by using satellite-based precipitation data in African catchments is that most, if not all, satellite precipitation products are geographically biased towards either underestimation or overestimation, despite some of them having good correlation with ground observations (i.e., Macharia *et al.*, 2022; Asadullah *et al.*, 2008; Dinku *et al.*, 2007). The lack of adequate ground precipitation observations makes it difficult to validate, as well as correct, the product's bias with an acceptable degree of certainty. There is not a single precipitation product that has been found to perform better than other precipitation products across African landscapes and southern Africa in particular (i.e., Macharia *et al.*, 2022). For the Luangwa Basin there is no guarantee that any of the precipitation products are spatially representative of a basin that is about 159,000 km^2 with varying topographical attributes. For instance, compared to point-based field observations of precipitation at six weather stations in Zambia (three stations in the Luangwa Basin and the other three outside of the Luangwa Basin) no single satellite-based precipitation product showed consistency with all weather stations (see Table A1 in the supplementary data). Using an ensemble of precipitation products is said to reduce errors and is therefore recommended (e.g.: Weerasinghe *et al.*, 2020; Asadullah *et al.*, 2008). When the annual mean of an ensemble of four satellite-based precipitation products was compared to annual means of field observations at different weather stations the margin of either underestimation or overestimation was reduced (See Table A1 in supplementary data). To this extent, for the general water balance, this study used annual mean of four satellite precipitation products. The four precipitation products are the Climate Forecasting System Reanalysis (CFSR), Climate Hazards Group Infra-Red Precipitation with Station data (CHIRPS), ECMWF Reanalysis v5 (ERA5) and TerraClimate (see Table 1). These satellite precipitation products were selected purely based on availability and the fact that they are spatially distributed and cover the entire Luangwa Basin (Table 1). Field observations of precipitation for GART Chisamba (data for the period 2020 – 2022) and Lusaka International Airport, Kabwe, Mwinilunga and Serenje weather stations for the years 2014 - 2016 were obtained from the Southern African Science Service Centre for Change and Adaptive Land Management (SASSCAL) weathernet (Last accessed: 20 January, 2023; <http://www.sasscalweathernet.org>). The observations for Mpika for the year 2021 were obtained from the ZAMSECUR project dataset

490

495

available at 4TU.ResearchData repository (<https://doi.org/10.4121/19372352.v2>) (Zimba *et al.*, 2022). Three weather stations, GART Chisamba, Lusaka International Airport and Mwinilunga, are outside of the Luangwa Basin and were used for comparison purposes only. However, GART and Lusaka International airport stations are very close to the Luangwa Basin. The other three stations Kabwe, Serenje and Mpika are within the Luangwa Basin (see Table A1 in the supplementary data for location coordinates of the weather stations). ~~However~~ Nevertheless, the results of the comparison of satellite precipitation products with field observations were similar (underestimation or overestimation) at all weather stations both in the Luangwa Basin and outside the basin (See Table A1 in the supplementary data).

Estimating runoff data

Reliable monthly basin-scale field observations of runoff were only available for the period 1961 -1992 and not for the study period 2009 – 2020. Monthly modelled TerraClimate runoff data (Abatzoglou *et al.*, 2018) was available for the period 1958 – 2020. Compared to field observations TerraClimate runoff data was significantly higher during the peak rainfall period of January-February. At annual scale TerraClimate overestimated runoff data but strongly correlated ($r = 0.83$) with field observations (Fig. 4a).

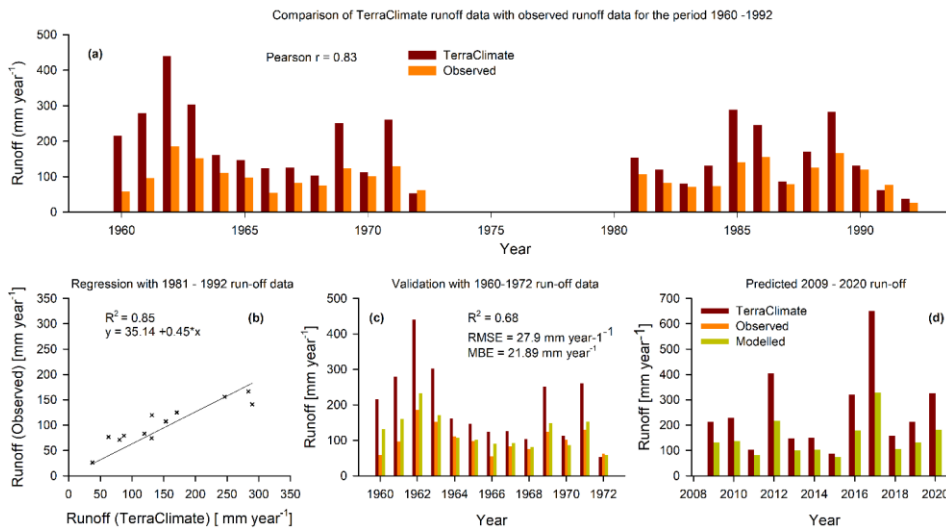


Figure 4: Procedure for extending near field observations runoff data for the period 2009-2020 using the TerraClimate runoff data as the predictor.

Based on the correlation of annual TerraClimate runoff data with field observations a linear regression equation was formulated to help generate extended near field observations time series for the period 2009-2020. TerraClimate runoff data was used as predictor variable. The TerraClimate runoff data was used because of availability free of cost and with relatively fine temporal and spatial resolution (monthly and 54 km respectively) (Table 1). Firstly, the field

540 observations runoff data and TerraClimate runoff data for the period 1960 - 1992 were split into two segments, 1960 - 1972 and 1981 - 1992. The runoff data for the period 1981 -1992 was used as training data to generate a linear equation with the TerraClimate runoff data as the predictor variable (Fig. 4b). The generated linear equation was validated using the 1961-1972 TerraClimate runoff data as a predictor variable (Fig. 4c). The predicted 1961-1972 runoff data with the TerraClimate runoff data as a predictor variable was then compared to the field observations for the same period (Fig. 4 c). The performance statistics of the equation showed $R^2 = 0.68$, $RMSE = 27.9 \text{ mm year}^{-1}$ and mean bias error (MBE) = $21.9 \text{ mm year}^{-1}$ (Fig. 4 c). The linear regression equation was then used to generate near field observations runoff data for the period 2009 – 2020 with TerraClimate runoff data for the same period as the predictor variable (Fig. 4 d). Generally, both for the observed and extended time series (with TerraClimate data as predictor) the annual runoff coefficient was 11%. The near field observations extended runoff data was then used in the water balance approach, as explained in Section 2.2.4 Eq. (1)5, to estimate actual evaporation at basin level.

555 2.2.5 Time series pre-processing and Statistical analyses

560 Before performing statistical analyses, the original time series of evaporation, LAI, NDVI, Soil moisture and air temperature, were adjusted for seasonality. The centred moving average (CMA) and adjusted seasonal factor (ASF) approach was used to deseasonalise the time series (Ghysels, Osborn, and Rodrigues, 2006; Nelson *et al.*, 1999; Briuinger, Krishnaiah, and Cleveland, 1983).

The coefficient of variation ($CVC_{\bar{x}}$) (%) in Eq. (2) (Helsel *et al.*, 2020) was used to understand the extent to which the satellite-based evaporation estimates varied between each other for each phenophase. Furthermore, the analysis of variance (ANOVA) (Helsel *et al.*, 2020) and all pairwise multiple comparison procedures with the Tukey Test (Helsel *et al.*, 2020) were performed. The pairwise comparison assisted in observing the satellite-based evaporation estimates that were significantly similar or different in magnitudes in each phenophase. The correlations (similarity in temporal trends) among satellite-based evaporation estimates were assessed at monthly and annual scales using a non-parametric technique: the Kendal correlation test (Helsel *et al.*, 2020).

$$570 \quad CVC_{\bar{x}} = \frac{\bar{x}}{\bar{s}} \quad (2)$$

575 where \bar{x} is mean of the observations and \bar{s} the standard deviation. The higher the $CVC_{\bar{x}}$ value, the larger the standard deviation compared to the mean, which implies greater variation among the variables. To establish the extent to which the satellite-based evaporation estimates underestimated or overestimated evaporation, relative to E_{wb} , the mean bias error (Eq. 3) is used:

$$580 \quad MBE = \frac{1}{n} \sum_{i=1}^n (E_{S_i} - E_{a(wb)_i}) \quad (3)$$

where n is the number of annual data used, $E_{a(wb)}$ is the water balance-based actual evaporation time series and E_s is the satellite-based evaporation estimates time series. The smaller the mean

Formatted: Font: Not Bold

Formatted: Font: Not Bold

Formatted: Indent: First line: 1.27 cm

Formatted: Font: Not Bold

Formatted: Font: Italic

Formatted: Font: Not Bold

bias error value (positive or negative), the less the deviation of the predicted values from the water balance obtained values (Helsel *et al.*, 2020).

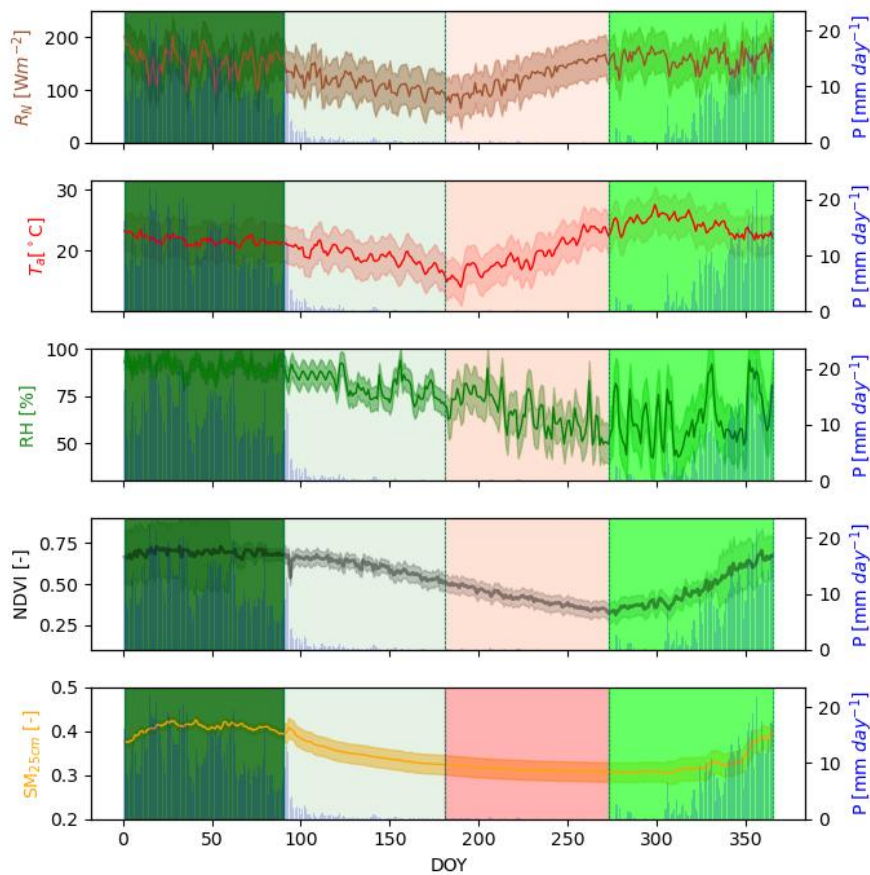
585 **3 Results and discussion**

3.1 Basin scale miombo woodland climate and phenological temporal trend(s)

Figure 5 shows Luangwa Basin miombo woodland (area delineated miombo woodland only in Fig. 1b) aggregated 2009-2020 MODIS NDVI and CFSR data climate conditions: net radiation (R_N), air temperature (T_a), relative humidity (RH), soil moisture (SM) and precipitation (P). The peak atmospheric and phenological variables values were observed in the early and mid-rainy seasons during the green-up and maturity/peak phenophases. The lowest values in atmospheric and phenological variables were observed in the cool dry season during the green-down and dormant phenophases. Net radiation, air temperature, relative humidity covaried (positively or negatively) with the NDVI (proxy for canopy phenology) depending on the phenophase (Fig. 5 and Fig. A2 in the supplementary data).

590

595



600

605

610

615

620

625

630

Figure 5: Luangwa Basin miombo woodland spatially and temporally aggregated 2009-2020 daily atmospheric conditions: net radiation (R_N), precipitation (P), relative humidity (RH) and air temperature (T_a); phenological conditions proxied by the NDVI; and soil moisture (SM). The shaded areas represent the phenophases as used in this study: January – March is the peak/maturity, April – June is the senescence/green-down, July – September is the dormant and October – December is the green-up/mid-green-up phenophase. Shaded area for variables is the standard deviation. DOY is the day of the year.

The strong correlation between climate and phenology (i.e., NDVI and air temperature/soil moisture) in the miombo woodland (Fig. A2 in the supplementary data) agreed with observations made by Chidumayo (2001) and in other ecosystems (Pereira *et al.*, 2022; Niu *et al.*, 2013; Cleland *et al.*, 2007).

Formatted: Left, Indent: First line: 0 cm, Space After: 8 pt, Line spacing: Multiple 1.08 li, Hyphenate

645

3.2 Observed phenological conditions in the miombo woodland

650 It was observed that the canopy closure is varied, ranging between 2 percent to about 70 percent in the shrub, dry miombo woodland and wet miombo woodland (Fuller, 1999). Therefore, depending on location and dominant species, exposure of the understory, field, and ground layers to incident solar radiation through the canopy is substantial (Fig. 6, Chidumayo, 2001; Fuller, 1999).



Figure 6: Dry season (a) and rainy season (b) tree layer, understory, and field layer conditions at the wet miombo woodland site in Mpika, Zambia. Images taken on 29th September and 23rd December, 2021.

670

The field layer during the rainy season mainly comprises green grass (Fig. 6b and Chidumayo, 2001). Therefore, total LAI and NDVI in phenophases in the rainy season can be largely attributed to both the field layer i.e., grass, understory, and the tree layer, i.e.: shrubs and tree canopy (i.e., Fig. 6b and Chidumayo, 2001). In the dry season, the grass in the field layer and some understory non-deep rooting shrubs dry out (Fig. 6a and Chidumayo, 2001, Fuller, 1999). Therefore, the changes in total LAI and NDVI in the phenophases in the dry season can largely be attributed to the changes in the tree layer of the miombo species (i.e., Fig. 6a, Fig. 7 and Chidumayo, 2001).

675

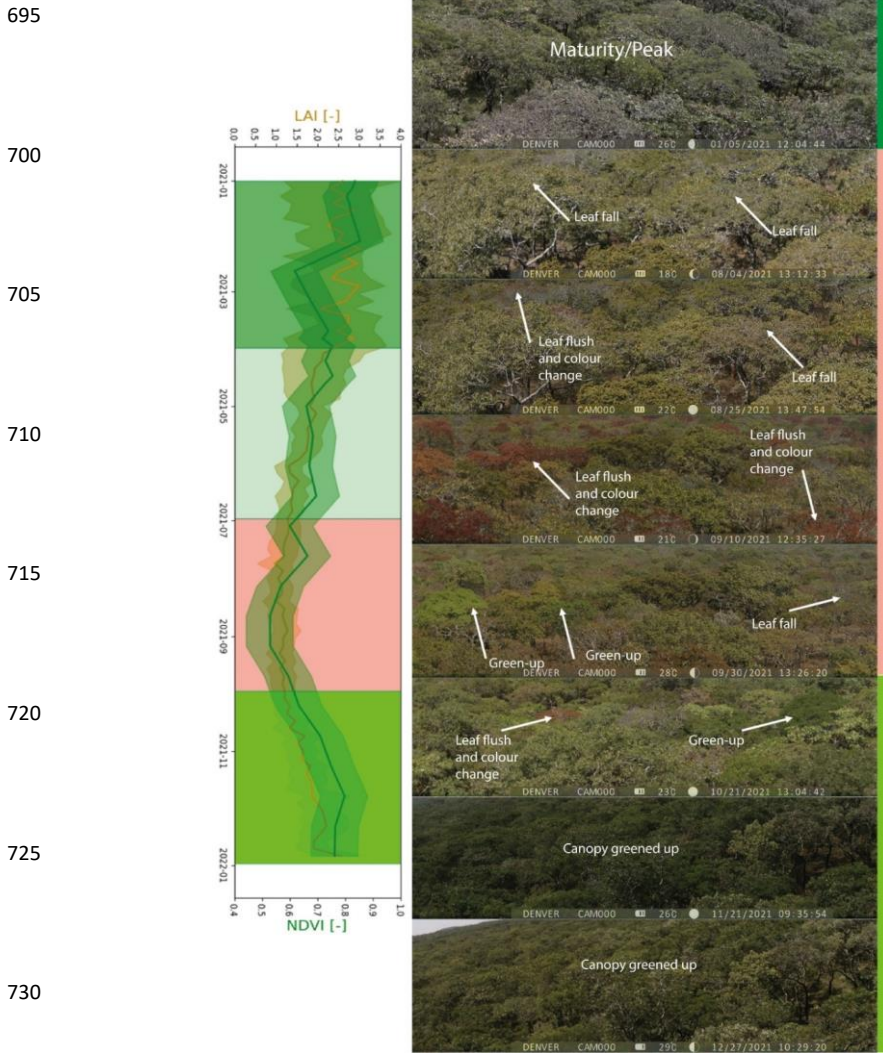
The LAI and NDVI were used as proxies to observe the changes in the canopy cover across different phenophases of the miombo woodland. At [a 27.7km-by-27.7km grid pixel-scale \(Fig. 8a\)](#) the spatial distribution and mean values of the LAI and NDVI for the wet miombo woodland differed with that for the dry miombo woodland (Fig. 8a). This difference is due to the differences in species composition and distribution at each site. Furthermore, there are differences in soil type, soil moisture, temperature, nutrients, rainfall, and canopy closure at the two sites (i.e., Chidumayo, 2001; Fuller, 1999). However, trends in the NDVI and LAI across different phenophases of the miombo woodland at the two sites were similar ([Pearson \$r = 0.73\$ for LAI and NDVI respectively](#)) (Fig. 8b). Highest LAI and NDVI, both in the dry miombo woodland and wet miombo woodland, were observed in the maturity/peak phenophases during the mid-rainy season (January – March) (Figs. 5, 7 & [8bc and Fig. A3 in the supplementary data](#)). [This period for peak LAI and NDVI \(Figs. 7 & 8\) agrees with Chidumayo \(2001\) who observed that peak green biomass in the miombo](#)

680

685

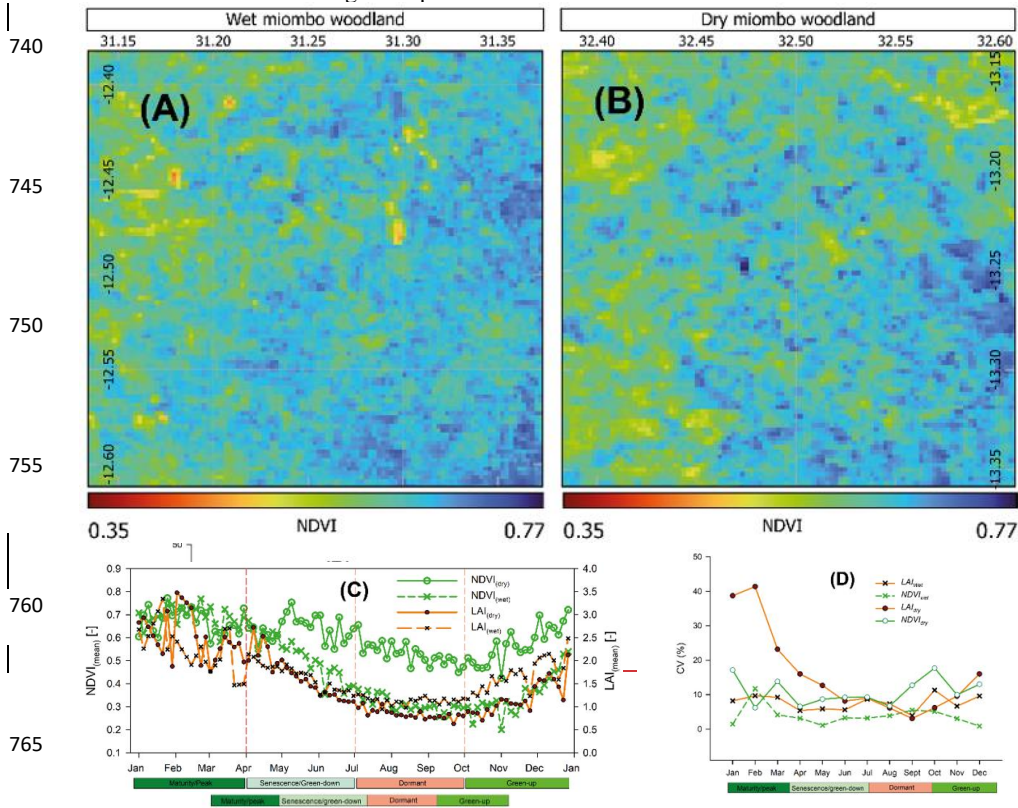
690

woodland occur anytime between January and May. The lowest LAI and NDVI were observed in the dormant phenophase in August/September during the warm pre rainy season (Figs. 5, 7 & 8).



735 **Figure 7:** Temporal trend of MODIS LAI, NDVI, and the wet miombo woodland canopy display trend for the year 2021 at Mpika study site. Shaded area are phenophases: January – March is the

Maturity/Peak; April-June is the Senescence/Green-down; July-September is the Dormant while October – December is the green-up. Shaded area for variables is the minimum and maximum.



Formatted: Tab stops: 9.71 cm, Left

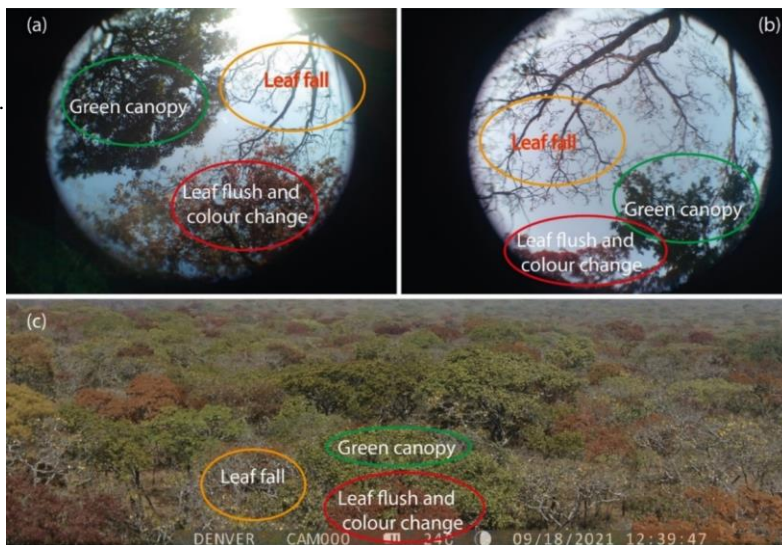
Table 2. Dormant phenophase CV correlation

| Variables | LAI _(wet) | NDVI _(wet) | LAI _(dry) | NDVI _(dry) |
|-----------------------|----------------------|-----------------------|----------------------|-----------------------|
| LAI _(wet) | 1 | | | |
| NDVI _(wet) | -1.00 | 1 | | |
| LAI _(dry) | 0.98 | -0.98 | 1 | |
| NDVI _(dry) | -0.75 | 0.75 | -0.69 | 1 |

Figure 8: Spatial distribution of NDVI at the (A) wet miombo woodland and (B) dry miombo woodland site for the period January-December, 2021. (C) Temporal distribution of the LAI and NDVI for the wet miombo woodland and dry miombo woodland. (D) Coefficients of variation in the LAI and NDVI values at the wet miombo woodland and dry miombo woodland in the Luangwa Basin in Zambia for the year 2021.

785 This period for peak LAI and NDVI (Figs. 7 & 8) agrees with Chidumayo (2001) who
observed that peak green biomass in the miombo woodland occur anytime between January and
May. The lowest LAI and NDVI were observed in the dormant phenophase in August/September
during the warm pre-rainy season (Figs. 5, 7 & 8).

790 The leaf-fall, leaf-flush and changes in colour of the leaves intensifies in the August-
795 September period (Fig. 7, Chidumayo, 2001; Chidumayo and Frost, 1996; Fuller, 1999). The
intensified leaf-fall, leaf-flush and leaf colour changes may also explain the
increased variations in the NDVI values in August-September (Fig. 8d). Table 2 shows the
correlation coefficients of the coefficients of variations in NDVI and LAI values for the dry
miombo woodland and wet miombo woodland.



820 **Figure 9:** Heterogeneity in leaf-fall and leaf-flush activities among miombo
woodland species: observed from under the canopy (a, b) and as observed above the canopy (c).
825 Images taken at the wet miombo woodland site in Mpika, Zambia. Images taken on 18
September, 2021.

825 The coefficients of variation in LAI and NDVI values for the dry and wet miombo
woodland were only similar for the dormant phenophase (Pearson $r = 0.98$ and 0.75 for the LAI
and NDVI respectively (Fig. 8 and Table 2). This similarity in the dormant phenophases may be
due to the plants undergoing similar phenological processes; leaf-fall and leaf-flush. In the

dormant phenophase the grass component would have dried out, leaving the tree component (i.e., the canopy) to determine the leaf area (Chidumayo, 2001).

830 The coefficients of variation of LAI values in July and August over the wet miombo woodland can be attributed to increased leaf-fall activity (Fig. 8). Fuller (1999) observed that in the wet miombo woodland the co-simultaneous occurrence of leaf-fall and leaf-flush, in August and September, resulted in net zero change in the canopy closure. The net zero change increase in canopy closure may explain the observed low coefficient of variation of the LAI values in 835 September (Fig. 8). The high coefficient of variations of LAI and NDVI values, for both dry miombo woodland and wet miombo woodland, during the mid-rainy season in the maturity/peak phenophase can be attributed to two factors: firstly, the heterogenous growth of the green biomass of the woodland which occurs anytime between January and May (Chidumayo, 2001, Fuller, 1999) and the effect of cloud cover on the quality of the satellite-based LAI and NDVI products (Vermote and Wolfe, 2015; Zang *et al.*, 2003). Furthermore, the differences in the canopy closure between 840 the dry miombo woodland and wet miombo woodland (Fuller, 1999) may be the reason for differences between the coefficients of variations in LAI and NDVI values in the maturity/peak and senescence/green phenophases. For instance, the dry miombo woodland, which has a lower canopy closure compared to the wet miombo (Fuller, 1999), is likely to have a higher grass component. Additionally, the differences in miombo species composition, distribution of rainfall, 845 soil type and soil moisture, among other variables, may result in varied phenological differences between the dry miombo woodland and wet miombo woodland (Chidumayo, 2001; Fuller, 1999).

However, unlike in the other phenophases, there appeared strong correlations (Table 2) in the variations in LAI and NDVI values in the dry miombo woodland and wet miombo woodland in the dormant phenophase. The simultaneous occurrence of leaf fall and leaf flush (see Fig. 9) is one of the phenological attributes that distinguishes the miombo woodland from other woodlands (Fuller, 1999; White, 1983). The leaf fall and leaf flush in the dry season (Figs. 7 & 9) occur many weeks and even months before the start of the rains. The growth of the new leaves in the dry season is sustained by both access to deep soil moisture, including ground water, and the adapted plant water storage mechanism (i.e., Tian *et al.*, 2018; Vinya *et al.*, 2018; Fuller, 1999; Savory, 1963). The leaf fall and leaf flush occur simultaneously (see Fig. 9) and result in net zero change increase in canopy closure during the dry season in the wet miombo woodland (i.e., Mpika) (Fig. 9 and Fuller, 1999). The balance in the leaf fall and leaf flush may explain the lower coefficient of variation in LAI values in September in both dry miombo woodland and wet miombo woodland. Therefore, in the dormant phenophase and the early green up in October, when the total LAI and NDVI can largely be attributed to the miombo woodland plants, the trends in the phenology appear to be similar in both dry and wet miombo woodland, though at different levels (Fig. 8).

Formatted: Highlight

Commented [hz1]:

865 3.3 Phenophase-based difference in satellite-based evaporation estimates

3.3.1 Correlation of satellite-based evaporation estimates

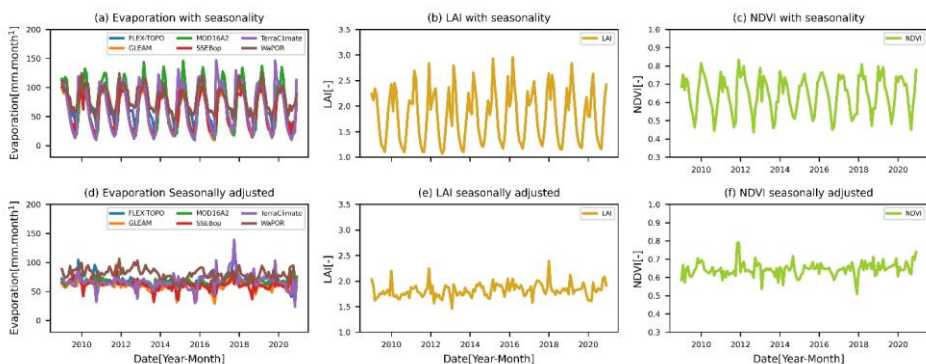
870 Figure A3 in the supplementary data shows the temporal distribution of evaporation in relation to the proxy of woodland canopy cover (i.e., NDVI) and rainfall across phenophases in a hydrological year of the Luangwa Basin. The highest satellite-based evaporation estimates were observed during the rainy season (with highest NDVI values) while the lowest were in the dry season (with lowest NDVI values) (Fig. A3 in the supplementary data).

Time series of satellite-based evaporation products and proxies (LAI and NDVI) for woodland canopy cover for the Luangwa Basin miombo woodland were adjusted for seasonality

(Fig. 10). The original time series and the seasonally adjusted time series for the dry miombo woodland and wet miombo woodland are shown in Fig. A4 in the supplementary data.

For analysis the data were segmented based on climate phenophases and satellite-based (NDVI) phenophases (Fig. 2 and as described in Section 2.2.11-13). ~~cascaded binned~~ ~~With reference to both non-stationary and stationary time series, in different phenophases, each satellite-based evaporation estimate appeared to correlate differently with other evaporation estimates (Figs. 11, 12 and Figs. A4 – A7 in the supplementary data). For instance, in the warm dry season/dormant phenophase, FLEX-Topo and WaPOR had generally lower correlations with the rest of the satellite-based evaporation estimates (Figs. 11, 12 and Figs A4 – A7 in the supplementary data). In the rainy season/maturity/peak phenophase the SSEBop showed most lower correlations with other satellite-based evaporation estimates.~~

~~With both non-stationary time series (with seasonality) and stationary (deseasonalised) time series significantly (Figs. 10) stronger correlations among the satellite-based evaporation products were observed during the rainy season and the cool dry season (Figs. 10, 11 and 12). Weaker correlations were observed during the warm dry season. Stronger correlation among satellite-based evaporation products appears to be during periods with high tree leaf area, soil moisture and vegetation water (Figs. 5 and 7) during the rainy season and cool dry season (Figs. 11 and 12) and lowest during water stressed period(s) (Figs. 5 and 7) in the warm dry season (Figs. 11 and 12). Generally, compared to time series with seasonality, the deseasonalised time series gave lower correlations among the satellite-based evaporation products across seasons and phenophases (Figs. 10, 11 and 12). The same pattern of correlation observed for the miombo woodland at the Luangwa Basin scale was observed for the dry miombo woodland and wet miombo woodland (Figs. xxxxx in the supplementary data)~~



~~maturity phenophase in the rainy season.~~

920

Figure 10. Original non-stationary time series and seasonally adjusted (deseasonalised) time series for the miombo woodland in the Luangwa Basin: aA, dD is the evaporation, Bb, eE is the LAI and Cc, Ff is the NDVI.

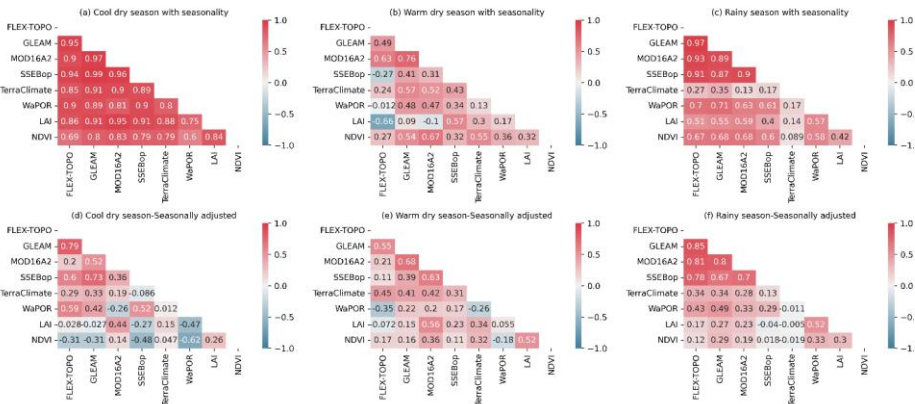
925

With reference to both non-stationary and stationary time series, in different phenophases, each satellite-based evaporation estimate appeared to correlate differently with other evaporation estimates (Figs. 11, 12 and Figs. A45 – A87 in the supplementary data). For instance, in the warm dry season/dormant phenophase, FLEX-Topo and WaPOR had, generally, lower correlations with the rest of the satellite-based evaporation estimates (Figs. 11, 12 and Figs. A45 – A78 in the supplementary data). In the rainy season/maturity/peak phenophase the SSEBop showed most lower correlations with other satellite based evaporation estimates.

930

The satellite evaporation estimates showed largest correlation coefficients in the warm dry season/green up phenophase and cool dry season/senescence/green down phenophases (Figs. 11, 12 and Figs. A4 – A7 in the supplementary data).

935

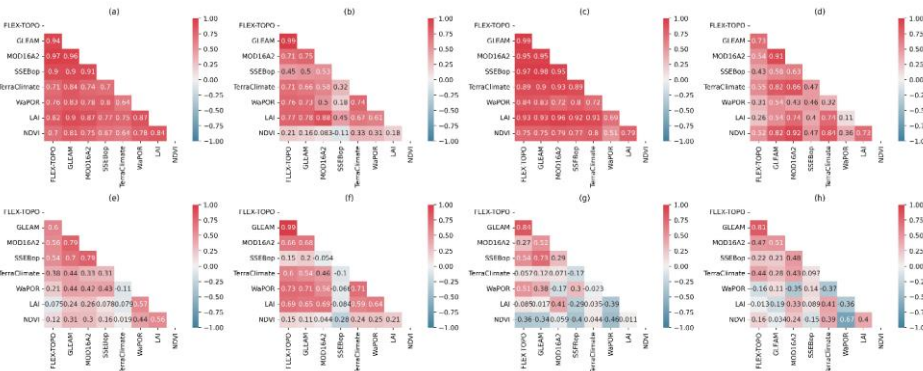


940

Figure 11. Climate-based phenophases correlation of satellite-based evaporation products estimates and proxies (LAI and NDVI) for woodland canopy cover for the miombo woodland in the Luangwa Basin: (a)-(c) original non-stationary time series with seasonality, (d) – (f) seasonally adjusted time series.

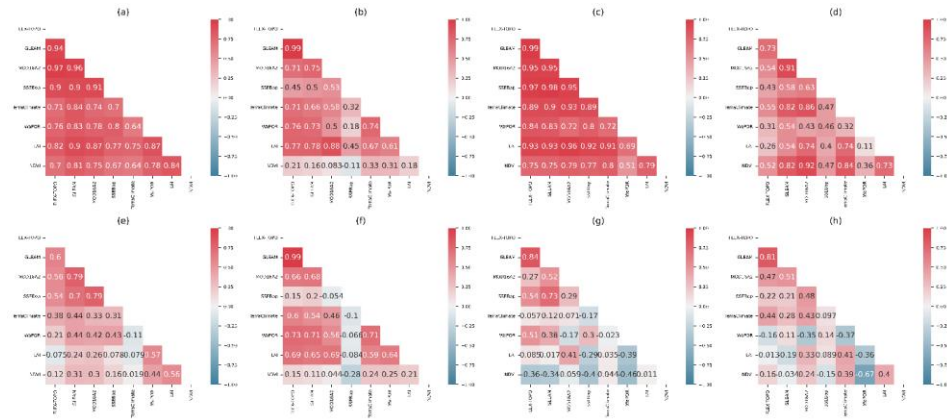
945

950



955

960



down/mid-green-down, (a, n) dormant.

965

~~In the rainy season/maturity/peak phenophase the SSEBop showed most lower correlations with other satellite based evaporation estimates. The satellite evaporation estimates showed largest correlation coefficients in the warm dry season/green up phenophase and cool dry season/senesence/green down phenophases (Figs.11,12 and Figs. A5 – A8 in the supplementary data).~~

970

However, with both non-stationary time series (with seasonality) and stationary (seasonally adjusted) time series, significant stronger ($r > 0.5$, $p\text{-value} < 0.05$) correlations among the satellite-based evaporation estimates were observed during the rainy season and immediately after the rains in the cool dry season (Figs. 10, 11 and 12). Significant weaker ($r < 0.5$, $P\text{-value} < 0.05$) correlations were observed during the warm dry season/dormant phenophases (Figs.11,12 and Figs. A5 - A8 in the supplementary data).

975

Stronger correlations among satellite-based evaporation estimates appears to be during periods with high woodland leaf area, high soil moisture content and high vegetation water during the rainy season and cool-dry season (Figs. 5, 7, 11 & 12). The same pattern of correlation of satellite-based evaporation estimates observed for the miombo woodland at the Luangwa Basin scale was observed for both the dry miombo woodland and wet miombo woodland (Figs. A5 – A8 in the supplementary data).

980

To the contrary, the lowest correlation coefficients among satellite-based evaporation estimates appear to be during water stressed period(s) in the warm dry season (Figs. 5, 7, 11 & 12). Generally, compared to time series with seasonality, the seasonally adjusted time series gave lower coefficients of correlation among the satellite-based evaporation estimate across seasons and phenophases (Figs. 11, 12).

985

~~Furthermore, the coefficients of variation of evaporation estimates showed that larger differences in the magnitudes (i.e., means) of evaporation of the satellite based evaporation estimates were largest in the warm dry season (i.e., $CV = 49\%$ and 11% for the non-stationary and seasonally adjusted time series respectively) (Fig. 13 & 14).~~

990

~~Stronger correlation and lower differences in the magnitudes of evaporation estimates among satellite based evaporation estimates appears to be during periods with high woodland leaf~~

area, high soil moisture content and high vegetation water (Figs. 5 and 7) during the rainy season and cool dry season (Figs. 11 and 12). To the contrary, the lowest correlation coefficients of satellite based evaporation estimates appear to be during water stressed period(s) (Figs. 5 and 7) in the warm dry season (Figs. 11 and 12). Generally, compared to time series with seasonality, the seasonally adjusted time series gave lower coefficients of correlation among the satellite based evaporation products across seasons and phenophases (Figs. 10, 11 and 12). The same pattern of correlation of satellite based evaporation estimates and coefficients of variation in the mean estimates of evaporation observed for the miombo woodland at the Luangwa Basin scale was observed for both the dry miombo woodland and wet miombo woodland (Figs. A34 – A78 in the supplementary data).

3.3.2 Temporal variations in satellite-based evaporation estimates across phenophases

Across phenophases (climate and satellite-based) comparison of the means of the seasonally adjusted time series of satellite-based evaporation estimates did not show large differences ($< 0.5\%$ difference) in the coefficients of variation of estimates (Figs. 13, 14 & Fig. A9 in the supplementary data). It appears that when seasonality is removed the means of satellite-based evaporation estimates show minimal different across phenophases with relatively higher coefficients of variation in the warm dry season phenophase/dormant phenophase and cool dry season/senescence phenophase (Figs. 13, 14 & Fig. A9 in the supplementary data).

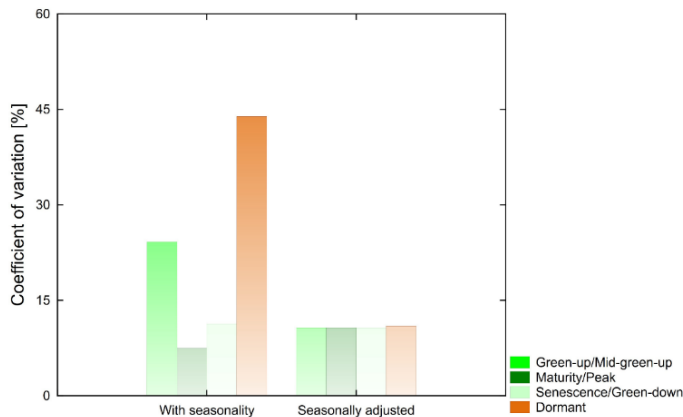


Figure 13. Satellite data-based phenophases coefficients of variation of estimates of satellite-based evaporation estimates for non-stationary time series and seasonally adjusted time series for the miombo woodland in the Luangwa Basin.

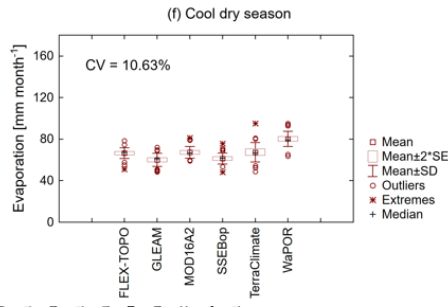
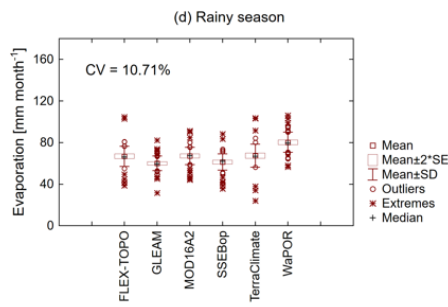
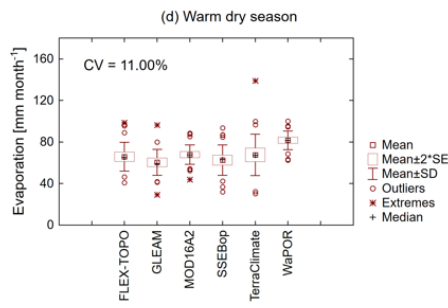
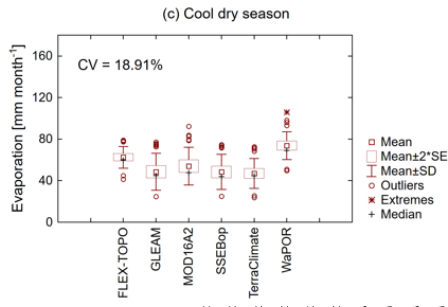
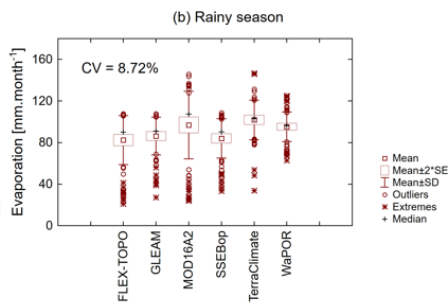
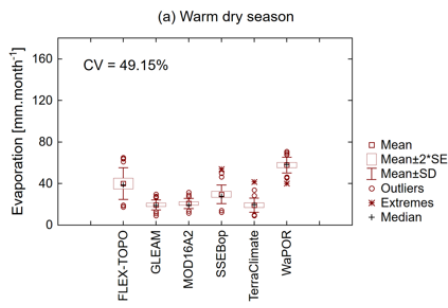
Formatted: Indent: First line: 1.27 cm

Formatted: Font: Bold

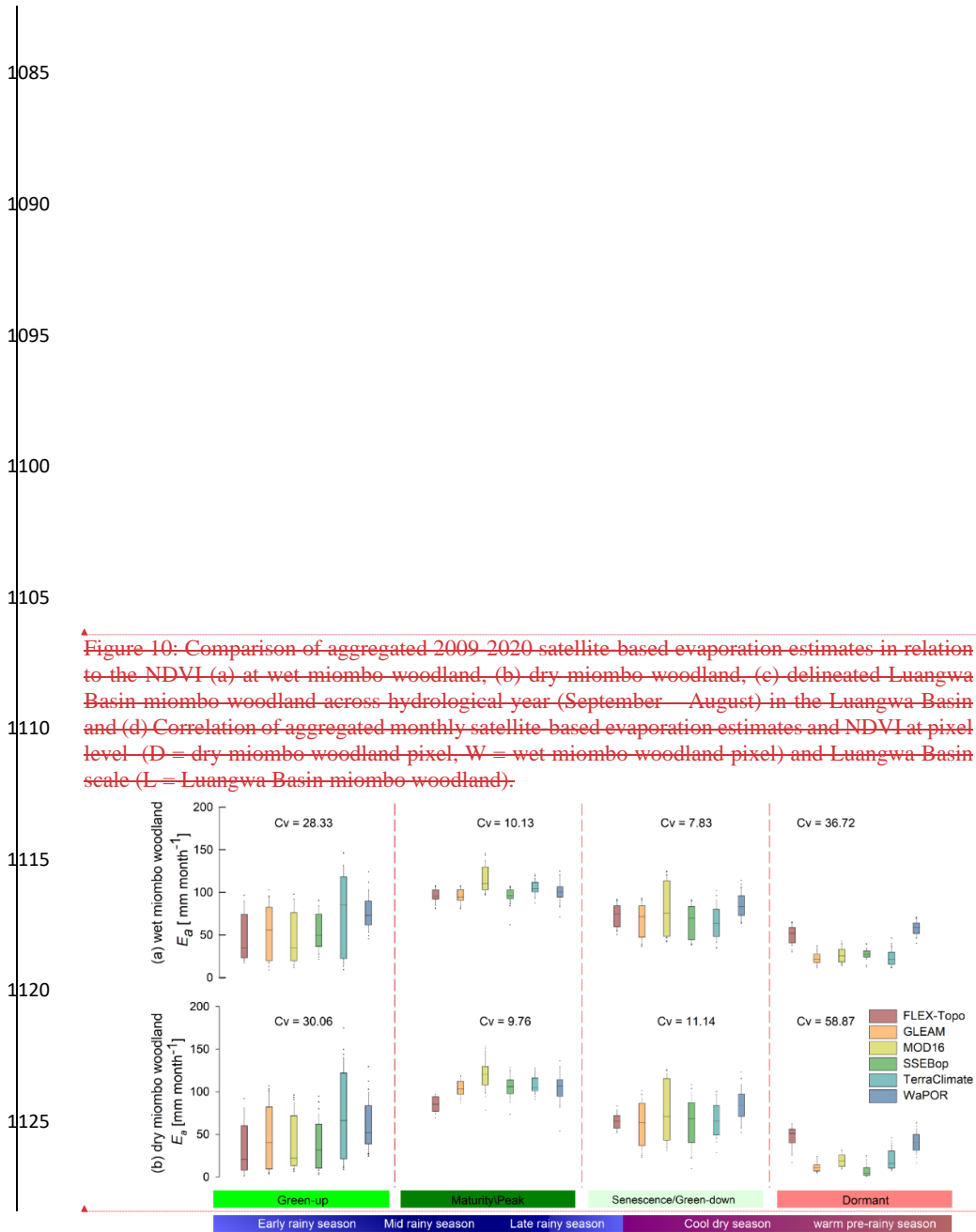
Formatted: Font: Bold

Formatted: Indent: First line: 0 cm

1040
1045
1050
1055
1060
1065
1070
1075
1080



Formatted: Indent: First line: 0 cm



Formatted: Font: Not Bold

Formatted: Font: Not Bold

1130 Figure 14: Box plots Comparison of satellite-based evaporation estimates, (a-c) with
seasonality and (c-f) with seasonally adjusted time series, across climate-based phenophases based
on hydrological year (a) in wet miombo woodland and (b) in dry miombo woodland of the miombo
woodland for the period 2009 - 2020 in the Luangwa Basin. The coefficient of variation (CV) is
for the comparison between the six satellite-based evaporation estimates.

1135 The dry season coefficients of variations in evaporation estimates could be indicative of
the possible influence of the adapted water limited conditions buffering mechanisms by the
miombo species. Across phenophases the WaPOR showed the highest estimates of evaporation
while GLEAM consistently showed the lowest mean estimates (Fig. 14 d- f). For instance, the
1140 canopy cover at the wet miombo woodland (Figs. 7 & 9) remained high (i.e., as evidenced in the
satellite-based NDVI mean values of around 0.55 in Fig. 7). With the highlighted adapted attributes
of the miombo species for the dry season it is probable that inadequate representation in satellite-
based evaporation estimates could result in varied estimates of transpiration.

1145 Furthermore, time series with seasonality showed significant differences in the coefficients
of variation between phenophases with the largest observed in the warm dry season (i.e., CV =
49.15 %; 43.90 % for the warm dry season and dormant phenophases respectively) (Fig. 13, 14 &
Fig. A9 in the supplementary data). ~~It appears that when seasonality is removed the means of~~
~~satellite-based evaporation estimates are not significantly different similar across phenophases~~
~~though the coefficients of variation for the warm dry season phenophase/dormant phenophase and~~
~~cool dry season/senescence phenophase are slightly higher than that for the other phenophases~~
1150 (Figs. 13 & 14). ~~With reference to time series with seasonality, for the warm dry season/dormant~~
~~phenophase, the meaning of the lower coefficients of correlation and higher coefficient of variation~~
~~(i.e., 49.15 %) is that, could indicate that while the temporal trends among some of the satellite-~~
~~based evaporation estimates are similar (r > 0.5) (Figs. 11 & 12), the amounts of evaporation~~
~~estimates are also significantly different (CV > 40%) (Figs. 13, 14 & Fig. A9 in the supplementary~~
~~data) (Figs. 13 & 14). The occurrence in the warm dry season of higher coefficients of variation,~~
~~with both non-stationary times series and seasonally adjusted time series, consolidates the possible~~
~~role of the adapted phenological and physiological attributes of miombo species on evaporation.~~

1160 In contrast, for the rainy season/~~green-up~~/maturity/peak phenophase, except for the
SSEBop and TerraClimate, the temporal trends among satellite-based evaporation estimates ~~we~~
are largely similar ($r > 0.5$) and the magnitudes of evaporation estimates ~~are~~ not very different (CV =
8.72 %; 7.46% for the rainy season and maturity/peak phenophases respectively) (Figs. 11, 12, 13,
& 14 & Fig. A9 in the supplementary data).

Compared to the warm dry season

1165 the cool dry season/senescence/green-down phenophases showed higher correlations ($r >$
5) and lower differences in the magnitudes of estimates of satellite-based evaporation estimates
(CV = 18.9 %, 101.297% for the cool dry season phenophase and senescence/green-down
phenophase respectively) (Figs. 11, 12, 13, 14 & Fig. A9 in the supplementary data) (Figs. 11, 12,
13 & 14). The results for the senescence/Green-down phenophase appear to agree with the findings
1170 by Zimba *et al.* (2023) in which they showed, at point scale, that for these phenophases the
temporal trends and magnitudes of satellite-based evaporation estimates were similar to each other
and also to the field observations of actual evaporation in the wet miombo woodland.

In the dormant phenophase, FLEX Topo and WaPOR had, generally, lower correlations
with the rest of the satellite-based evaporation estimates (Fig. A3 in the supplementary data). In

Formatted: Indent: First line: 1.27 cm

1175 the maturity/peak phenophase in the rainy season MOD16 and SSEBop showed most lower
1180 correlations with other satellite based evaporation estimates. The green up phenophase and
senescence/green down phenophase showed higher correlation coefficients ($r > 0.6$) among all
satellite based evaporation estimates (Fig. A3 in the supplementary data).

1185 Substantial differences in the means of satellite based evaporation estimates, at both pixel
level in the dry wet miombo woodland, wet miombo woodland and at the Luangwa Basin miombo
1190 woodland scale, were observed during the green up ($C_v = 28.23; 30.06; 22.63$ percent,
respectively) and dormant phenophase ($C_v = 36.72; 58.87; 39.98$ percent, respectively) (Figs. 10,
11 & Table A3 in the supplementary data). For the green up phenophase, the meaning of the
coefficients of correlation and variation in evaporation estimates is that, while the trends among
the satellite based evaporation estimates are similar, the amounts are significantly different. In
contrast, for the maturity/peak phenophase the trends among some satellite based evaporation
estimates are not similar (Fig. A3 in the supplementary data) but the magnitudes are similar (Fig.
11). For the senescence/green down phenophase both the trends and magnitudes of satellite based
evaporation estimates are similar. The results for the senescence appear to agree with the findings
1195 by Zimba *et al.* (2023) in which they showed, at point scale, that the temporal variation and
magnitudes of satellite based evaporation estimates were similar to each other and also to the field
observations of actual evaporation in the wet miombo woodland.

1200 For the dormant phenophase most of the trends and magnitudes of satellite based
evaporation estimates were significantly different. Most variations in actual evaporation estimates
among the satellite based evaporation estimates were observed in the dormant and green up
phenophases (see Fig.11). In the warm dry season/-dormant phenophase in the dry season the
FLEX-Topo and WaPOR, followed by FLEX-Topo, showed higher estimates of evaporation
1205 compared to other satellite based evaporation estimates (Figs. 11 a, b4 & A3, A9 in the
supplementary data). Zimba *et al.* (2023) showed, at point scale in the wet miombo woodland, that
satellite based evaporation estimates underestimated actual evaporation in the warm dry season.
They also showed that while the NDVI was generally in a downward trajectory from May to
September, the observed actual evaporation had a rising trajectory which was in agreement
with the rising air temperature and net radiation. Compared to other satellite based estimates the
WaPOR followed the same temporal trend as the field observations of actual evaporation of the
1210 wet miombo woodland in the dry season (Zimba *et al.*, 2023). In this study, FLEX-Topo and
WaPOR showed negative correlation with the LAI/NDVI in the warm dry season/dormant
phenophases in the dry season (Figs. A3 in the supplementary data, 11d, e, & 12g, h). Therefore,
with reference to findings by Zimba *et al.* (2023) and Figs. 11 & A3 12 in the supplementary data,
FLEX-Topo and the WaPOR appear to have the correct temporal variation trend of actual
evaporation of the miombo woodland in the cool dry season/ senescence/green-down and the warm
dry season/dormant phenophases in the dry season.

1215 The green-up phenophase is at the start of the rainy season with increasing LAI and high
canopy cover (i.e., mean NDVI between 0.5 and 0.7) and highest net radiation (i.e., 150 Wm^{-2})
(Figs. 5, 7 & 9 & 10). The dormant phenophase is during the driest part of the year with the lowest
moisture in the topsoil, least -woodland canopy cover (i.e., NDVI ≈ 0.5) but, compared to the
senescence/green-down phenophase, with increasing net radiation and air temperature (Figs. 5, 7
& 9).

1220 What is important to note is that, unlike during the maturity/peak and senescence/green
down phenophases, the total LAI and total NDVI during the dormant and early green-up
phenophases can largely be attributed to the tree layer (i.e., miombo woodland canopy) (Fig. 6:

Formatted: Not Highlight

Formatted: Not Highlight

Formatted: Not Highlight

Formatted: Not Highlight

Formatted: Not Highlight

Chidumayo, 2001; Chidumayo and Frost, 1996). The implication of the total LAI and NDVI in the dry season is that the dormant and early green-up phenophases are likely to be more representative of the evaporation of the miombo species than the other phenophases in the rainy season, and early dry season (cool dry season) when the green grass component is substantially increases high. Compared to the maturity/peak and the senescence/green-down phenophases, the dormant and green-up phenophases showed higher coefficients of variations in evaporation estimates among satellite-based evaporation estimates (Figs. 13 & 14 and Fig. A4 in the supplementary data).

The comparatively higher substantial differences (i.e., coefficients of variations (Figs. 13 & 14) in the estimates) in of satellite-based evaporation estimates during the dormant and green-up warm dry season phenophases suggests that there are aspects of the evaporative processes (i.e., adapted phenological and physiological water interactions) attributes of the miombo species that are possibly not taken into account in satellite-based evaporation estimates. The possible explanations for the observed temporal trends variation (i.e., correlations) and coefficients of variations in the satellite-based evaporation estimates are given in section 3.85.

3.3.3 Spatial distribution of satellite-based evaporation estimates across phenophases

Figure 15 shows spatial-temporal distribution of satellite-based evaporation estimates across different phenophases for the hydrological year 2019/2020. The comparison was based on the entire Luangwa Basin, including non-miombo woodland regions. Generally, the spatial distribution and detail of evaporation estimates are different, but, like the temporal trends, they are most pronounced in the dormant and green-up phenophases (Figs. 13, 14 & 15). During periods of high soil moisture and high leaf area (i.e., Figs. 5 & 7), in the maturity/peak and senescence/green-down phenophases, the products are more in agreement. It can further be seen that during the dormant phenophase, all six evaporation estimates showed higher actual evaporation in wooded areas (Fig. 15) (refer to Fig. 1 b, c for the cover of the miombo woodland in the Luangwa Basin). Potential contributing factors to the observed differences in spatial-temporal distribution of satellite-based evaporation estimates are highlighted in section 3.5.

Formatted: Not Highlight

Formatted: Not Highlight

Formatted: Not Highlight

Formatted: Not Highlight

Formatted: Not Highlight

Formatted: Not Highlight

Formatted: Not Highlight

Formatted: Not Highlight

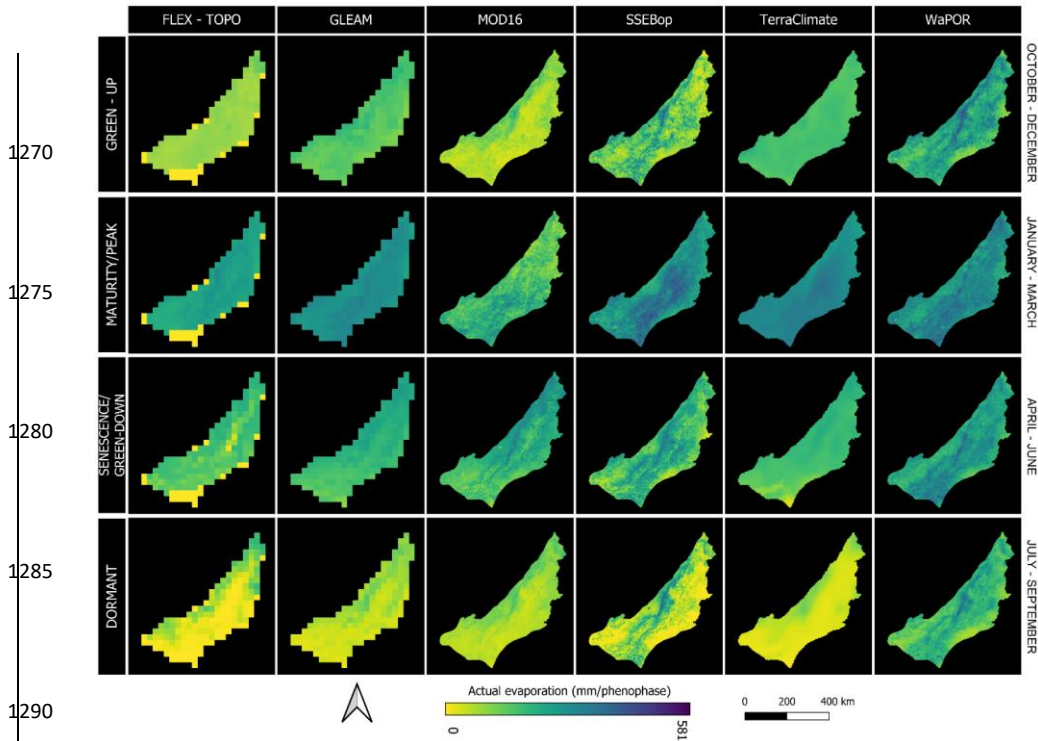


Figure 15: Spatial-temporal distribution of satellite-based evaporation estimates across different vegetation phenophases of the Luangwa Basin for the hydrological year September 2019 - August 2020.

3.3.44 Pairwise multiple comparison of satellite-based evaporation estimates at Luangwa Basin miombo woodland scale

It appeared there are no statistically significant differences in the estimates of evaporation for the dry miombo woodland and wet miombo woodland by each satellite-based evaporation estimate (Fig. A910 and Tables A42 in the supplementary data). ~~shows a summary of results of the ANOVA. Therefore, the all pairwise comparison was performed only for the entire miombo woodland of the Luangwa Basin, and all (Tables A4 and A5 in the supplementary data) shows the results of the all pairwise multiple comparison of satellite-based evaporation estimates with seasonality (Table A4) and the seasonally adjusted time series (Table A5 in the supplementary data). The six satellite-based evaporation estimates are compared with each other in each phenophase. The number of times each satellite-based evaporations estimate is different from the other five satellite-based evaporation estimates was observed as shown in Fig. 12.~~

~~The most differences in the means of satellite-based evaporation estimates appear to be in the rainy season (Green-up/Maturity/Peak phenophases) and the warm-dry season (dormant phenophase). For both time series, it appears appeared the WaPOR estimates were the most different across phenophases (Fig. 16). The other satellite-based evaporation estimates with mean estimates significantly different from~~

other estimates, after the WaPOR, are the FLEX-Topo, followed by the MOD16 and TerraClimate (Fig. 16, Tables A4 & A5 in the supplementary data). In the dormant phenophase the magnitudes of FLEX Topo and WaPOR were similar to each other but significantly (p value < 0.05) different from the other satellite based estimates. In the same phenophase GLEAM and MOD16 showed similar temporal variation and magnitudes. SSEBop estimates were significantly different from MOD16 and TerraClimate estimates. The rest of the comparisons did not show significant differences in magnitudes of satellite based evaporation estimates (Table A4 in the supplementary data). During the green up phenophase there were no significant (p value > 0.05) differences between GLEAM estimates and FLEX Topo estimates. SSEBop estimates were significantly (p value < 0.05) different from FLEX Topo and MOD16 estimates. The TerraClimate and WaPOR estimates were significantly different (p value < 0.05) from other estimates (Table A4 in the supplementary data). In the maturity/peak phenophase MOD16 was significantly different (p value < 0.05) from the other satellite based evaporation estimates. During the same period GLEAM, SSEBop and WaPOR were significantly different from at least one other satellite based estimate (Table A4 in the supplementary data).

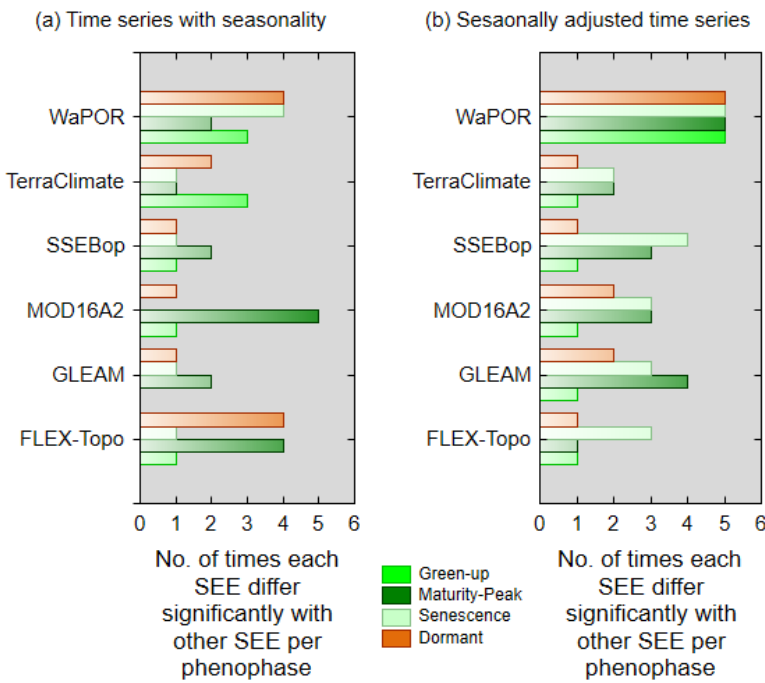


Figure 16: Number of times each satellite-based evaporation estimate (SEE) was significantly different to one or more other SSE in each phenophase at Luangwa Basin miombo woodland scale.

Formatted: Indent: First line: 0 cm

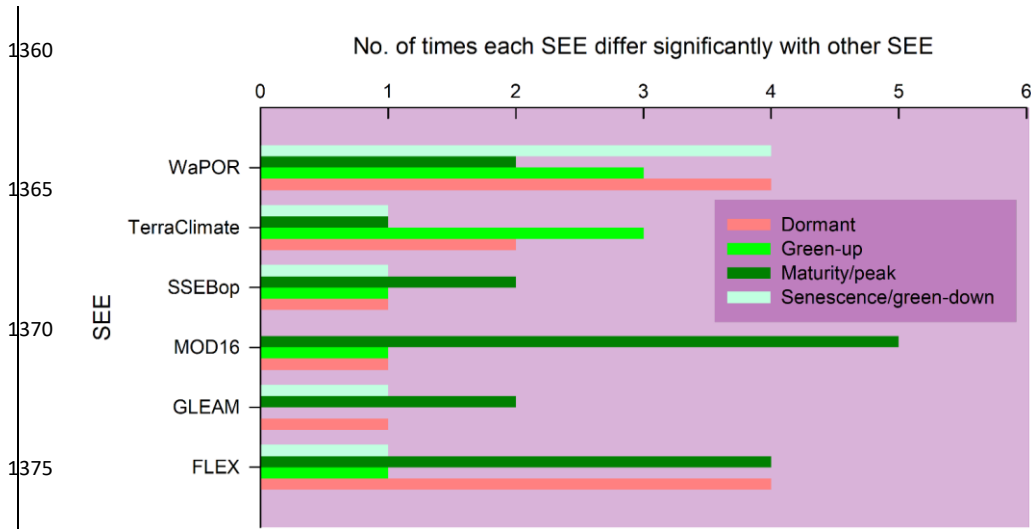


Figure 12: Number of times each satellite-based evaporation estimate (SEE) was significantly different to one or more other SSE in each phenophase at Luangwa Basin miombo woodland seale.

During the senescence/green-down phenophase the WaPOR significantly differed with FLEX Topo, GLEAM, SSEBop and TerraClimate while the rest of the comparison showed similarity in magnitudes among satellite-based evaporation estimates. Across phenophases WaPOR showed the highest frequency of being significantly different from other satellite-based evaporation estimate followed by FLEX Topo, MOD16 and TerraClimate (Fig. 12 and Table A4 in the supplementary data).

3.3.55 Variations within each climate, LAI, NDVI and satellite-based evaporation estimate

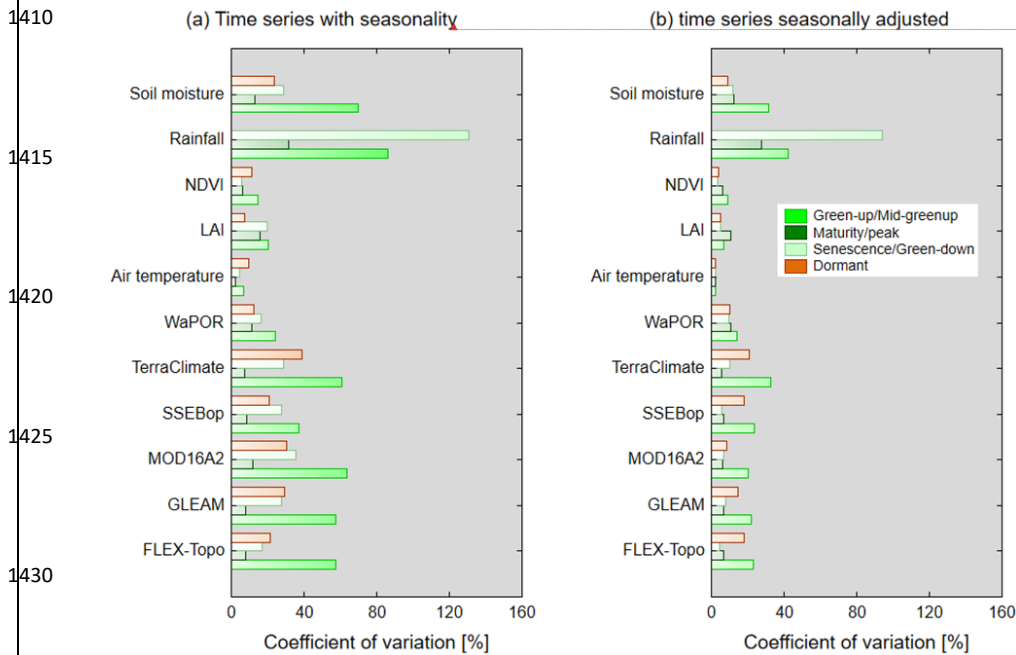
With the exception of WaPOR, ~~(temporal or spatial??. I guess temporal)~~ monthly temporal variations of satellite-based evaporation estimates were highest during the green-up phenophase, followed by the dormant and senescence/green-down phenophases (Fig. 13a7). The maturity/Peak showed the lowest coefficients of variations of ~~of satellite of satellite~~-based evaporation estimates (Fig. 173a and Table A3 in the supplementary data). The green-up and senescence/green-down phenophases are at the boundaries of the dry season into the mid-rainy season (in case of green-up phenophase) and the rainy season into the dry season (in the case of the senescence/green-down phenophase). The coefficients of variation of the NDVI (i.e., canopy cover), rainfall (i.e., water availability) and temperature (i.e., energy availability) in the green-up and senescence/green-down phenophases (Fig. 13b167) likely explains the temporal variations in within each satellite-based evaporation estimates product (Table A3 in the supplementary data). The phenophases in which the LAI, NDVI, rainfall and soil moisture appear to show larger coefficients of variations are also the phenophases in which individual satellite-based estimates show higher coefficients of variation (Fig. 167). The temporal variation of satellite-based evaporation estimates in the dormant

Formatted: Left

Commented [HS2]: The reviewer was also confused. First of all. Does this comparison only refer to one pixel, or the entire basin, or only the dry or wet miombo? This is not clear. Is it then spatial variation or temporal? If it is temporal then what scale does it refer to? That is important to mention.

Commented [HZ3R2]: Monthly variations

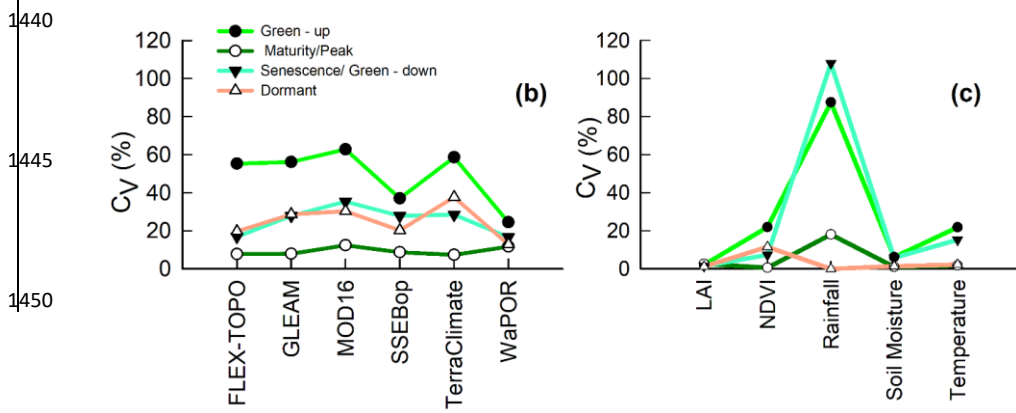
phenophase could be as a result of the changes in the canopy cover due to the leaf--fall, leaf--flush and leaf colour changes (i.e., NDVI as shown in Figs. 7, 9 & 17). Figure 176 generally shows that the variations in LAI, NDVI, rainfall, soil moisture and air temperature are mirrored in the variations of the satellite-based evaporation estimates.



Formatted: Font: Not Bold

The variations of satellite based evaporation estimates in the dormant phenophase could be due to the changes in the canopy cover (i.e., NDVI as shown in Fig. 13b) due to the leaf fall, leaf flush and leaf colour changes.

Commented [HS4]: The terms "within" are very confusing. I guess you mean that you did the statistical analysis exclusively for a certain time series. But you don't have to mention within there. So I deleted it. In the title of 3.5 it is ok.



1455

1460

Figure 1736: Coefficients of variations for (a) showing within satellite based evaporation estimate variations across phenophases and time series with seasonality and (b) seasonally adjusted time series within variations in estimates for atmospheric and phenological variables across phenophases for the miombo woodland at Luangwa Basin miombo woodland scale.

1465

In the dormant phenophase in the dry season FLEX Topo, SSEBop and WaPOR showed lower coefficients of variations compared to GLEAM, MOD16 and TerraClimate (Fig. 13a). The maturity/peak phenophase showed the lowest coefficients of variation of satellite based evaporation estimates, LAI, NDVI, rainfall, soil moisture and temperature (Fig. 13). Figure 13 generally shows that, among many other influencing factors, the variations in LAI, NDVI, rainfall, soil moisture and air temperature are mirrored in the variations of the satellite based evaporation estimates.

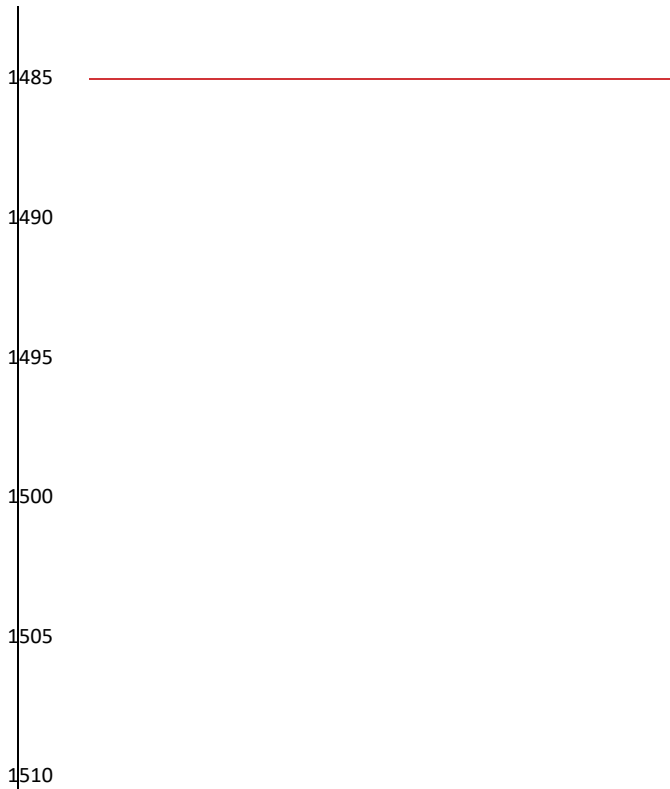
1470

3.6 Differences in spatial distribution of satellite based evaporation estimates

1475

Figure 14 shows spatial temporal distribution of satellite based evaporation estimates across different phenophases for the hydrological year 2019/2020. The comparison was based on the entire Luangwa Basin, including non miombo woodland regions. Generally, the spatial distribution and detail of evaporation estimates are different, but they are most pronounced in the dormant and green up phenophases (Fig. 14). During maturity/peak and senescence/green down the products are more in agreement. It can further be seen that during the dormant phenophase, all six evaporation estimates showed higher actual evaporation in wooded areas (Fig. 14) (refer to Fig. 1 b, c for the cover of the miombo woodland in the Luangwa Basin). Potential contributing factors to the observed differences in spatial temporal distribution of satellite based evaporation estimates are highlighted in section 3.8.

1480



Formatted: Indent: First line: 0 cm

Figure 14: Spatial temporal distribution of satellite based evaporation estimates across different vegetation phenophases of the Luangwa Basin for the hydrological year September 2019– August 2020.

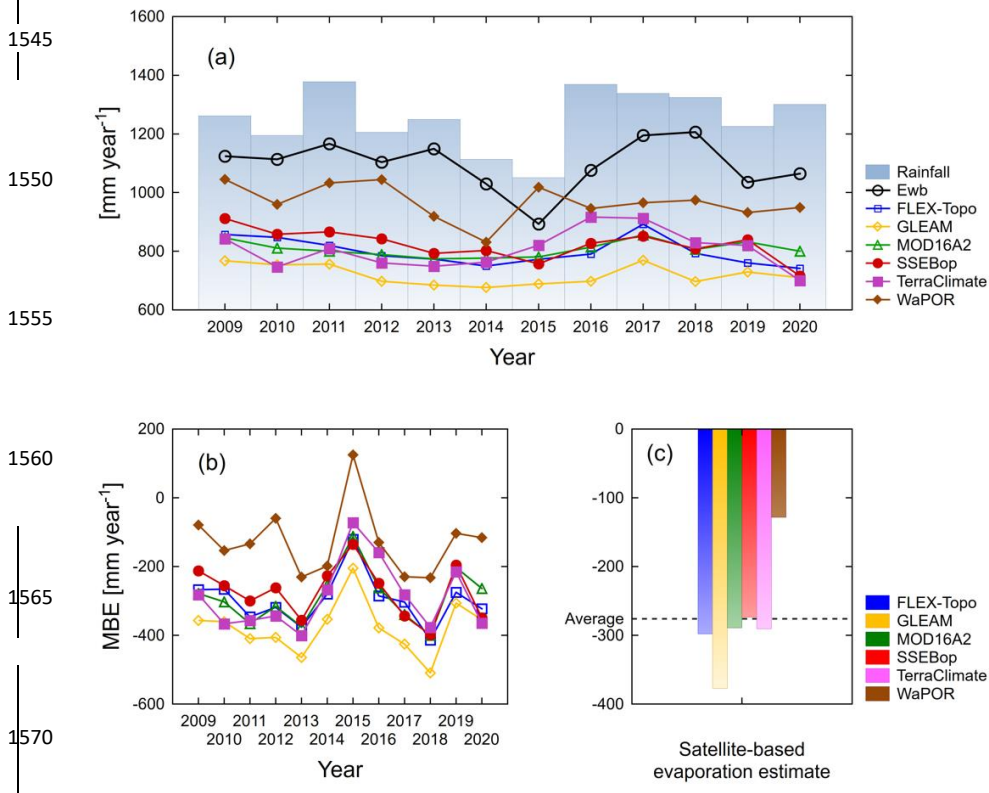
3.47 Comparison of satellite-based evaporation estimates to the water balance-based actual evaporation

Figure 1588 shows the temporal comparison of satellite-based evaporation estimates with the water balance-based actual evaporation of the Luangwa Basin for the hydrological years for the period September 2009 to August 2020. This comparison included non-miombo woodland areas. All satellite-based evaporation estimates showed insignificant correlation ($p\text{-value} > 0.05$) with the water balance-based actual evaporation (E_{wb}) (Fig. A59101 in the supplementary data). Compared to the E_{wb} estimates, all six satellite-based evaporation estimates underestimated actual evaporation (Fig. 1588a, b). The poor correspondence can be due to several factors.

Firstly, the disregard of over-year storage may explain the very low actual evaporation estimate in the dry year 2015. In that year the over-year storage should likely not be disregarded, and it is also possible that farmers in the cropland areas withdrew water from small dams. Taking these factors into account would have led to a higher actual evaporation estimate in 2015.

Secondly, the overall higher water balance-based actual evaporation may be due to the

disregard of potential inter-basin groundwater exchange, or leakage of groundwater to the Zambezi. Hulsman et al. (2021) estimated that this leakage on average could amount to 143 mm/y. Secondly, the overall higher water balance based actual evaporation may be due to the disregard of potential inter-basin groundwater exchange, or leakage of groundwater to the Zambezi. Hulsman et al. (2021) estimated that this leakage on average could amount to 143 mm/y. This amount would be enough to bridge the bias between WaPOR and the water balance based actual evaporation in Fig. 15c. Furthermore, there are uncertainties in the river discharge and the spatially averaged precipitation, which may have been over-estimated. The extended runoff time series with TerraClimate may have been overestimated resulting in underestimating the water balance based actual evaporation at basin scale. The assumption of overestimation of the extended runoff data is based on the validation results of the linear equation used to extend the runoff time series, which showed $RMSE = 27 \text{ mm year}^{-1}$ and $MBE = 21 \text{ mm year}^{-1}$. In any given year, WaPOR appeared to have the least underestimation with an average MBE of 120 mm year^{-1} , while GLEAM had the largest underestimation with an average MBE of 370 mm year^{-1} .



1575

1580

Figure 1588: (a) Comparison of satellite-based evaporation estimates to the water balance-based estimate of actual evaporation for the Luangwa Basin, and (b) comparison of the MBE of satellite-based evaporation estimates for each year, and (c) comparison of the multi-year average MBE of individual satellite-based evaporation estimates.

1585

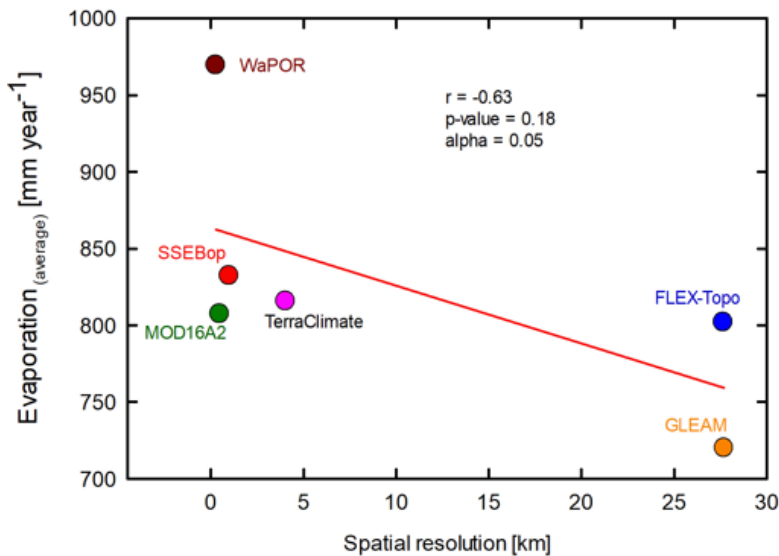
This amount would be enough to bridge the bias between WaPOR and the water balance-based actual evaporation in Fig. 18c. Furthermore, there are uncertainties in the river discharge and the spatially averaged precipitation, which may have been over-estimated.

The extended runoff time series with TerraClimate (Fig. 4 c, d) may have been overestimated resulting in underestimating the water balance-based actual evaporation at basin scale. The assumption of overestimation of the extended runoff data is based on the validation results of the linear equation used to extend the runoff time series, which showed RMSE = 27 mm year⁻¹ and MBE = 21 mm year⁻¹.

1590

In any given year, WaPOR appeared to have the least underestimation with an average MBE of 120 mm year⁻¹, while GLEAM had the largest underestimation with an average MBE of 370 mm year⁻¹ (Fig. 18c).

1595



1600

Figure 19. Luangwa Basin scale relationship between 2009-2020 annual averages of evaporation estimates and spatial resolution of satellite-based evaporation estimates.

1605

1610

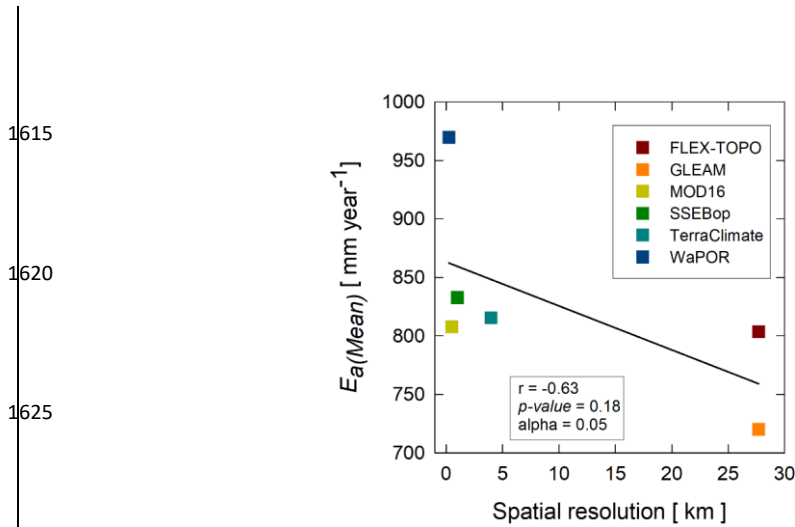


Figure 194896: Basin-scale relation between evaporation estimates and spatial resolution of satellite-based evaporation products.

At basin scale, it appeared there was no statistically significant correlation ($r = -0.63$; $p\text{-value} = 0.18$; $\alpha = 0.05$) between spatial resolution and evaporation estimates of each product (Fig. 194896). For instance, TerraClimate, with a coarser spatial resolution, showed similar bias estimates as SSEBop and MOD16. MOD16 had an even higher spatial resolution than SSEBop, but underestimated more. FLEX-Topo had a coarser spatial resolution than MOD16 and SSEBop but exhibited higher estimates in the warm dry season/dormant phenophases (July-September) (Figs. 10 and 11, 14 and Fig. A53, in the supplementary data). The lack of a clear relationship between spatial resolution and actual evaporation estimates (Fig. 194896), may imply that other factors such as the heterogeneity in the land cover (i.e., miombo woodland, mopane woodland, cropland, settlements etc), access to soil moisture and groundwater, differences in model structure (such as the inclusion of leakage), processes and model inputs, as highlighted in Zimba *et al.* (2023) and section 3.8.5 in this study, may be the largest contributing factors of the observed differences in the actual evaporation estimates at basin scale.

However, the underestimation of actual evaporation at basin scale by satellite-based evaporation estimates cannot be entirely attributed to the inaccuracies in the simulation of miombo woodland evaporation. The evaporation of other vegetation types, i.e., mopane woodland, has not been investigated. The basin scale water balance-based comparison suggests that satellite-based evaporation estimates possibly underestimate actual evaporation also in non-miombo woodland landscapes. This requires more investigation of different landscapes and land covers such as grassland, shrubland, wetland and mopane woodland. For a more comprehensive understanding of the evaporation of the Luangwa Basin there is need for the assessment of the phenology-water interactions of each vegetation type and the accompanying potential influence on the evaporation dynamics of the basin. Nevertheless, the results of this study agreed with Weerasinghe *et al.* (2020)

Formatted: No Spacing, Tab stops: Not at 6.86 cm

Formatted: No Spacing, Hyphenate

Formatted: No Spacing, Indent: First line: 0 cm, Hyphenate

Formatted: No Spacing, Hyphenate

Formatted: No Spacing, Justified, Tab stops: Not at 6.86 cm

Formatted: No Spacing, Tab stops: Not at 6.86 cm

Formatted: Font: Times New Roman, 12 pt

Formatted: Font color: Auto, Not Highlight

Formatted: Font: Times New Roman, 12 pt

Formatted: Font color: Auto, Not Highlight

Formatted: Font: Times New Roman, 12 pt

Formatted: Font: Times New Roman, 12 pt

Formatted: Font: Times New Roman, 12 pt

Formatted: No Spacing, Hyphenate

1660 who showed that most satellite-based evaporation estimates generally underestimate evaporation across African basins (i.e., Zambezi Basin). The lower underestimation by WaP~~A~~POR agreed with the point scale field observations for the wet miombo woodland (Zimba *et al.*, 2023) and suggests that Wa~~A~~POR is closest to actual evaporation of the miombo woodland in the Luangwa Basin.

1665 **3.5.8 Potential causes of differences in trends, magnitudes and spatial distribution of satellite-based evaporation estimates**

1670 Most pronounced differences in trends and magnitudes of satellite-based evaporation estimates of the miombo woodland have been observed in the dormant phenophase of the dry season (Figs. ~~10, 11, 12, 13, 14, 167~~ & A3 in the supplementary data). Evaporation during that period is dominated by transpiration (i.e., Tian *et al.*, 2018). The dominant phenological characteristic of the miombo species in the dry season is the co-simultaneous occurrence of leaf fall/leaf-fall, leaf flush/leaf-flush and greening up before commencement of seasonal rainfall (Figs. ~~7&9~~; Chidumayo and Frost, 1996; Frost, 1996) which affects transpiration (e.g., Marchesini *et al.*, 2015; Snyder and Spano, 2013). Tian *et al.* (2018) showed that the terrestrial groundwater storage anomaly (TWS) continued to decrease throughout the dry season and was indicative that miombo trees used deep ground water during that period. The suggestion that miombo trees access ground water is supported by Savory (1963) who showed that miombo species are deep rooting beyond 5 m with capacity to access ground water. Therefore, it is likely that satellite-based evaporation estimates using models whose structure, processes and inputs take into account the highlighted phenology-water interactions during the dry season and early rainy season, especially the access to deep soil moisture, would produce more accurate trends and magnitudes of evaporation in the miombo woodland.

Formatted: Not Highlight

Formatted: Not Highlight

1685 **3.5.8.1 Use of proxies for soil moisture**

1690 Some studies have shown that direct integration of soil moisture rather than the use of proxies improves the accuracy of actual evaporation estimates (Brust *et al.*, 2021; Novick *et al.*, 2016). The challenge with the use of proxies for soil moisture, for example in surface energy balance models, is that these are unable to fully account for changes in other factors that may influence sensible heat fluxes (Gokmen *et al.*, 2012). To improve the accuracy of estimation of water and energy fluxes in regions with recurrent plant water stress, such as in miombo woodland, Gokmen *et al.* (2012) suggested that the soil moisture be integrated in surface energy balance models. For instance, for MOD16 the use of the relative humidity and vapour pressure difference as proxies for soil moisture maybe a source of uncertainty in estimating transpiration (Novick *et al.*, 2016). Direct integration of soil moisture into the MOD16 algorithm appeared to improve the accuracy of actual evaporation estimates (Brust *et al.*, 2021). The energy balance-based SSEBop does not explicitly consider soil moisture dependency and assumes that the variations in satellite-based land surface temperature and vegetation indices, such as the NDVI, accounts for soil moisture (Senay *et al.*, 2013). TerraClimate uses the plant-extractable water capacity of soil for soil moisture input. However, the difficulty in determining the plant-extractable water capacity of the soil is in defining the extent of the rooting depth. GLEAM takes into account 2.5m of the sub-surface linked to observed precipitation. On the other hand, transpiration in FLEX-Topo and WaP~~A~~POR (ETLook model) is coupled to soil moisture in the root zone using an integrated approach.

Consequently, this may explain why the pairwise comparison showed that trends and magnitudes of FLEX-Topo and WaPOR were not significantly ($p\text{-value} > 0.05$) different (in both dry miombo woodland and wet miombo woodland) during the dormant phenophase (Tables A3, A4 in the supplementary data). Therefore, the integration of soil moisture in evaporation simulation and the accuracy of the soil moisture product used is likely to affect the accuracy of satellite-based transpiration estimates.

Formatted: Not Highlight

Formatted: Not Highlight

3.5.82 Optimisation of the rooting depth

Optimising rooting depth rather than the use of a standard depth has been shown to increase transpiration of trees in landscapes with a dry season (Kleidon and Heimann, 1998). Modifying rooting depth can improve energy flux simulations at both field scale and regional scale (Liu *et al.*, 2020). Wang-Erlandsson *et al.* (2016) showed that accurate root zone storage estimates “improved evaporation simulation overall, and in particular during the least evaporating months in sub-humid to humid regions with moderate to high seasonality”. Their study demonstrated that several forest types have developed rootzone storage mechanisms that help buffering for dry season conditions. Some miombo species are deep rooting, beyond 5 metres, while the soil moisture in the miombo woodland increases with depth (i.e., Chidumayo, 2001; Savory, 1963). Therefore, one of the potential causes of the observed differences in satellite-based evaporation estimates could be the rooting depth used in the simulation of evaporation. The satellite-based evaporation estimates used in this study are likely not to have optimised rooting depth for the miombo woodland as there are few studies in the public domain that have investigated the optimum rooting depth for effective simulation of transpiration of miombo woodland. Since ecosystems have adapted to local climatic conditions (Tian *et al.*, 2018), global scale root storage estimates and optimisation may not be able to effectively capture the climatic conditions at local and region scales.

3.5.3 Differences in landcover products used

The landcover proxies in satellite-based evaporation estimates may also explain the observed differences in both temporal and spatial distribution of evaporation. For instance, the MOD16 uses a global landcover product (Gray *et al.*, 2019; Running *et al.*, 2019) which had shown to misclassify certain land cover types and showed low user accuracy in certain regions (i.e., Leroux *et al.*, 2014). WaPOR uses the Copernicus land cover product, but adds the distinction between irrigated and rain-fed areas (FAO, 2018). For the vegetation fraction, GLEAM uses MODIS MOD44B (Martens *et al.*, 2017; Miralles *et al.*, 2011). Other satellite-based evaporation estimates (i.e., SSEBop) use vegetation indices such as the NDVI as proxy for vegetation cover.

Different vegetation types have different phenology-water interactions (i.e., Lu *et al.*, 2006) which influence actual evaporation (Forster *et al.*, 2022; Snyder *et al.*, 2013; Schwartz, 2013). Transpiration of the miombo woodland in the dry season is dependent on the landcover type and constrained by: root zone water availability (Wang-Erlandsson *et al.*, 2016; Gates & Hanks, 2015; Stancalie & Nert, 2012; Allen *et al.*, 1998), stomatal conductance thresholds and surface roughness, which are vegetation type and plant species dependent (i.e., Urban *et al.*, 2017; Wehr *et al.*, 2017; Gates & Hanks, 2015; Tuzet, 2011). Therefore, dissimilarities in the land cover products and their associated limitations possibly reflect in differences in the spatial-temporal distribution of satellite-based evaporation estimates.

3.8.5.4 Satellite-based rainfall products and rainfall interception

The differences observed in evaporation estimates may be related to differences in the quality of satellite-based precipitation products used and the ability of the models to effectively account for rainfall interception. Studies have shown that satellite precipitation products are geographically biased towards either underestimation or overestimation (i.e., Macharia *et al.*, 2022; Asadullah *et al.*, 2008; Dinku *et al.*, 2007). In the case of Africa, and southern Africa in particular, no single precipitation product has been found to perform better than other precipitation products across landscapes (i.e., Macharia *et al.*, 2022). The difference in precipitation products, with different spatial resolutions and accuracy levels, may explain the differences in the spatial-temporal distribution of satellite-based evaporation estimates during the rainy season. For instance, FLEX-Topo used the Climate Hazards Group Infra-Red Precipitation with Station data (CHIRPS) (Funk *et al.*, 2015), GLEAM used Multi-Source Weighted-Ensemble Precipitation (MSWEP) (Bai and Liu, 2018), which uses different algorithms, inputs and spatial resolution.

Rainfall interception is a function of vegetation cover, leaf area (LAI), spatial scale and precipitation. For instance, LAI influences canopy interception, throughfall and forest floor interception, and spatial and temporal scale influences the interception threshold (FAO, 2018; Gerrits, 2010; Savenije, 2004). Field observations showed that wet miombo woodland canopies intercepted up to 18-20 percent of rainfall annually (i.e., Alexandre, 1977). Therefore, differences in the quality and accuracy of land cover products, and even proxies such as the NDVI used for modelling interception, are likely to result in different evaporation estimates of evaporation products that have interception modules (i.e., FLEX-Topo, GLEAM, MOD16 and WaPOR).

4 Conclusions and recommendations

The study sought to find out to which extent a variety of satellite-based evaporation estimates were in agreement or differed in quantifying miombo woodland evaporation during its typical phenophases and to establish the underlying factor(s) for the discrepancies that emerged. The study also compared the different evaporation estimates to the annual water balance-based evaporation at basin scale. The following were the conclusions:

Non-stationary time series All satellite-based evaporation estimates strongly showed strong similarity in temporal trends between satellite-based evaporation estimates and correlated with the changes in phenology (proxied by the LAI and NDVI) in the green-up and senescence/green-down phenophases. Weaker correlations in temporal trends of satellite-based evaporation estimates and changes in phenology were observed in the dormant phenophase and the maturity/peak phenophase, but showed relatively weak correlations in the dormant and maturity/peak phenophases. Seasonally adjusted time series did not show strong similarity in temporal trends between satellite-based evaporation estimates and the changes in phenology, though the WaPOR showed relatively higher negative correlation values with the NDVI and LAI in the senescence/green-down phenophase and dormant phenophase in the dry season.

Both non-station time series and seasonally adjusted time series appeared to show weaker correlation correlations and high coefficients of variation among satellite-based evaporation estimates were observed in the dormant phenophase during the dry season warm dry season. Therefore, the observed differences in satellite-based evaporation estimates in the dry season appear to be due to limited understanding and inadequate representation of the

phenology-water interactions, that are influenced by the adapted physiological attributes such as the deep rooting and vegetation water storage of the miombo species.

1795 It is possible that the underestimations of satellite-based evaporation estimates₂ compared
to the water-balance based evaporation estimates₂ are affected by the disregard of over year storage
1800 in the deeper groundwater and the export of groundwater by leakage to the downstream Zambezi
River. Another cause for the discrepancy is the inadequate representation of the phenology-water
interactions of the miombo species, but also of other vegetation types such as the mopane
woodland. Consequently, field observations of evaporation across the different phenophases and
strata of the miombo woodland are required to obtain a comprehensive overview of the
characteristics of the actual evaporation of the ecosystem. This information can be used to help
improve satellite-based evaporation assessments in the Luangwa Basin and the miombo region as
whole.

1805 Finally, in view of the unique phenology, whereby evaporation starts before the onset of
rainfall, and the ability of the miombo species to access additional moisture stocks, inclusion of
these traits is likely to improve estimates of transpiration of the miombo woodland in the dry
season.

1810 **Author contribution**

Conceptualization, H.Z.; formal analysis, H.Z., P.H.; resources, H.S.; supervision, M.C.-G. and
1815 B.K.; writing—original draft, H.Z.; writing—review and editing, M.C.-G., B.K., H.S., P.H., I.N.,
and N.V. All authors have read and agree to the published version of the manuscript.

Funding

This study was conducted with the financial support of the Dutch Research Council (NWO) under
1820 the project number W 07.303.102.

Acknowledgements

This study is part of the ZAMSECUR Project, which focuses on observing and understanding the
remote water resources for enhancing water, food and energy security in Lower Zambezi Basin
1825 We wish to thank the Water Resources Management Authority (WARMA) in Zambia for the field
discharge data used in this study.

Conflict of interest:

1830 At least one of the (co-)authors is a member of the editorial board of Hydrology and Earth System
Sciences.

References

1835 Abatzoglou, J. T., Dobrowski, S. Z., Parks, S. A., & Hegewisch, K. C.: TerraClimate, a high-
resolution global dataset of monthly climate and climatic water balance from 1958-2015.

Scientific Data, 5, 1–12. doi:10.1038/sdata.2017.191, 2018.

Abrams, M., & Crippen, R.: ASTER Global DEM (Digital Elevation Mode) - Quick Guide for V3. *California Institute of Technology*, 3(July), 10, 2019.

1840 Allen R., G., Pereira L. S., Raes D, Smith M.: Crop evapotranspiration - guidelines for computing crop water requirements. FAO irrigation and drainage paper 56, Rome, Italy <http://www.fao.org/docrep/X0490E/X0490E00.htm>, 1998.

Alexandre, J.: Le bilan de l'eau dans le miombo (forêt claire tropicale). *Bulletin de la Société Géographie du Liège* 13, 107-126, 1977.

1845 Asadullah, A., McIntyre, N., & Kigobe, M.: Evaluation of five satellite products for estimation of rainfall over Uganda. *Hydrological Sciences Journal*, 53(6), 1137–1150. doi:10.1623/hysj.53.6.1137, 2008.

1850 Bai, P. and Liu, X.: Intercomparison and evaluation of three global high-resolution evapotranspiration products across China, *J. Hydrol.*, 566, 743–755, <https://doi.org/10.1016/j.jhydrol.2018.09.065>, 2018.

1855 Beilfuss, R.: A Risky Climate for Southern African Hydro ASSESSING HYDROLOGICAL RISKS AND A Risky Climate for Southern African Hydro, (September). doi:10.13140/RG.2.2.30193.48486, 2012.

Biggs, T., Petropoulos, G. P., Velpuri, N. M., Marshall, M., Glenn, E. P., Nagler, P., & Messina, A.: Remote sensing of actual evapotranspiration from croplands. *Remote Sensing Handbook: Remote Sensing of Water Resources, Disasters, and Urban Studies*, 59-99, 2015.

1860 Bogawski, P., Bednorz, E.: Comparison and Validation of Selected Evapotranspiration Models for Conditions in Poland (Central Europe). *Water Resour Manage* 28, 5021–5038. <https://doi.org/10.1007/s11269-014-0787-8>, 2014.

1865 Bonnesoeur, V., Locatelli, B., Guariguata, M. R., Ochoa-Tocachi, B. F., Vanacker, V., Mao, Z., ... Mathez-Stiefel, S. L.: Impacts of forests and forestation on hydrological services in the Andes: A systematic review. *Forest Ecology and Management*, 433(June 2018), 569–584. doi:10.1016/j.foreco.2018.11.033, 2019.

1870 Brust, C., Kimball, J. S., Maneta, M. P., Jencso, K., He, M., & Reichle, R. H.: Using SMAP Level-4 soil moisture to constrain MOD16 evapotranspiration over the contiguous USA. *Remote Sensing of Environment*, 255(January), 112277. doi:10.1016/j.rse.2020.112277, 2021.

Briuinger, D R, P R Krishnaiah, and William S Cleveland. "Seasonal and Calendar Adjustment." *Handbook of Statistics* 3: 39–72, 1983.

1875

Formatted: Font: Times New Roman, 12 pt

Formatted: No Spacing, Indent: First line: 0 cm, Adjust space between Latin and Asian text, Adjust space between Asian text and numbers

Formatted: Font: Times New Roman, 16 pt

Formatted: No Spacing, Indent: First line: 1.27 cm, Adjust space between Latin and Asian text, Adjust space between Asian text and numbers

- 1880 Buchhorn, M.; Smets, B.; Bertels, L.; De Roo, B.; Lesiv, M.; Tsendbazar, N.E., Linlin, L., Tarko, A.: *Copernicus Global Land Service: Land Cover 100m: Version 3 Globe 2015-2019: Product User Manual*. Zenodo, Geneva, Switzerland. <https://doi.org/10.5281/zenodo.3938963>, 2020.
- Campbell, B., Frost, P., & Bryon, N.: miombo woodlands and their use: overview and key issues. In “The Miombo in Transition: Woodlands and Welfare in Africa. Ed: B. Campbell (Bogor, Indonesia: Center for International Forestry Research) p 1–6, 1996.
- 1885 Chen, Y., Xia, J., Liang, S., Feng, J., Fisher, J. B., Li, X., ... Yuan, W.: Comparison of satellite-based evapotranspiration models over terrestrial ecosystems in China. *Remote Sensing of Environment*, 140, 279–293. doi:10.1016/j.rse.2013.08.045, 2014.
- 1890 Chidumayo, E. N.: Climate and Phenology of Savanna Vegetation in Southern Africa. *Journal of Vegetation Science*, 12(3), 347. doi: 10.2307/3236848, 2001.
- Chidumayo, E. N., & Frost, P.: Population biology of miombo trees. In The miombo in transition: woodlands and welfare in Africa, Campbell, B. (ed.). Bogor (Indonesia): CIFOR, ISBN 979-8764-07-2, 1996.
- 1895 Chidumayo, E. N.: Phenology and nutrition of miombo woodland trees in Zambia. *Trees*, 9(2), 67–72. doi:10.1007/BF00202124, 1994.
- Cleland, E. E., Chuine, I., Menzel, A., Mooney, H. A., & Schwartz, M. D.: Shifting plant phenology in response to global change. *Trends in Ecology and Evolution*, 22(7), 357–365. doi:10.1016/j.tree.2007.04.003, 2007.
- 1900 Dinku, T., Ceccato, P., Grover-Kopec, E., Lemma, M., Connor, S. J., & Ropelewski, C. F.: Validation of satellite rainfall products over East Africa’s complex topography. *International Journal of Remote Sensing*, 28(7), 1503–1526. doi:10.1080/01431160600954688, 2007.
- 1905 Ernst, W. and Walker, B.H.: Studies on the hydration of trees in miombo woodland in South Central Africa. *Journal of Ecology* 61, 667-673, 1973.
- FAO.: *WaPOR Database Methodology: Level 1 Data. Remote Sensing for Water Productivity Technical Report: Methodology Series*. Retrieved from http://www.fao.org/fileadmin/user_upload/faoweb/RS-WP/pdf_files/Web_WaPOR-beta_Methodology_document_Level1.pdf, last accessed: 20 June, 2022, 2018
- 1910 Forrest, J., Inouye, D. W., & Thomson, J. D.: Flowering phenology in subalpine meadows: Does climate variation influence community co-flowering patterns? *Ecology*, 91(2), 431–440. doi:10.1890/09-0099.1, 2010.
- 1915 Forrest, J., & Miller-Rushing, A. J.: Toward a synthetic understanding of the role of phenology in ecology and evolution. *Philosophical Transactions of the Royal Society B: Biological Sciences*, 365(1555), 3101–3112. doi:10.1098/rstb.2010.0145, 2010.
- Forster, M. A., Kim, T. D. H., Kunz, S., Abuseif, M., Chulliparambil, V. R., Srichandra, J., &

- 1920 Michael, R. N.: Phenology and canopy conductance limit the accuracy of 20
evapotranspiration models in predicting transpiration. *Agricultural and Forest Meteorology*,
315(December 2021), 108824. doi:10.1016/j.agrformet.2022.108824, 2022.
- 1925 Friedl, M., Gray, J., Sulla-Menashe, D.: MCD12Q2 MODIS/Terra+Aqua Land Cover
Dynamics Yearly L3 Global 500m SIN Grid V006 [Data set]. NASA EOSDIS Land
Processes DAAC. Accessed 2023-03-30 from
<https://doi.org/10.5067/MODIS/MCD12Q2.006>, 2019.
- 1930 Frost, P.: *The Ecology of Miombo Woodlands*. (B. Campbell, Ed.), *The Miombo in Transition:
Woodlands and Welfare in Africa*. Bogor, Indonesia: Center for International Forestry
Research. Retrieved from
<http://books.google.com/books?hl=nl&lr=&id=rpildJJVdU4C&pgis=1>, last accessed: 20
June 2022, 1996.
- 1935 Fuller, D. O.: Canopy phenology of some mopane and miombo woodlands in eastern Zambia.
Global Ecology and Biogeography, 8(3–4), 199–209. doi:10.1046/j.1365-
2699.1999.00130.x, 1999.
- Fuller, D. O., & Prince, S. D.: Rainfall and foliar dynamics in tropical southern Africa: Potential
impacts of global climatic change on Savanna vegetation. *Climatic Change*, 33(1), 69–96.
doi:10.1007/BF00140514, 1996.
- 1940 Funk, C., Peterson, P., Landsfeld, M., Pedreros, D., Verdin, J., Shukla, S., Husak, G., Rowland,
J., Harrison, L., Hoell, A., & Michaelsen, J.: The climate hazards infrared precipitation with
stations - A new environmental record for monitoring extremes. *Scientific Data*, 2, 1–21.
doi: 10.1038/sdata.2015.66, 2015.
- 1945 García, L., Rodríguez, J. D., Wijnen, M., & Pakulski, I.: *Earth Observation for Water Resources
Management: Current Use and Future Opportunities for the Water Sector*. Washington, DC
20433: Washington, DC: World Bank. doi:10.1596/978-1-4648-0475-5, 2016.
- Gates, D. M., & Hanks, R. J.: Plant factors affecting evapotranspiration. *Irrigation of
Agricultural Lands*, 11, 506–521. doi:10.2134/agronmonogr11.c28, 2015.
- 1950 Gerrits, A.M.J.: The role of interception in the hydrological cycle. Dissertation Delft
University of Technology. ISBN: 978-90-6562-248-8
<http://resolver.tudelft.nl/uuid:7dd2523b-2169-4e7e-992c-365d2294d02e>, 2010.
- 1955 Ghysels, Eric, Denise R. Osborn, and Paulo M.M. Rodrigues. "Chapter 13 Forecasting Seasonal Time
Series." *Handbook of Economic Forecasting*. [https://doi.org/10.1016/S1574-0706\(05\)01013-X](https://doi.org/10.1016/S1574-0706(05)01013-X),
2006.
- Gokmen, M., Vekerdy, Z., Verhoef, A., Verhoef, W., Batelaan, O., & van der Tol, C.:
Integration of soil moisture in SEBS for improving evapotranspiration estimation under

Formatted: Indent: Left: 0 cm

- 1960 water stress conditions. *Remote Sensing of Environment*, 121, 261–274. doi:10.1016/j.rse.2012.02.003, 2012.
- Gray, J., Sulla-Menashe, D., & Friedl, M. A.: MODIS Land Cover Dynamics (MCD12Q2) Product. *User Guide Collection 6*, 6, 8. Retrieved from https://modis-land.gsfc.nasa.gov/pdf/MCD12Q2_Collection6_UserGuide.pdf, last accessed: 20 June 2022, 2019.
- 1965
- Guan, K., Eric F. Wood, D. Medvigy, John. Kimball, Ming. Pan, K.K. Caylor, J. Sheffield, Xiangtao. Xu, and O.M. Jones.: Terrestrial hydrological controls on land surface phenology of African savannas and woodlands. *Journal of Geophysical Research: Biogeosciences*, 119(8), 1652–1669. doi:10.1002/2013JG002572, 2014, 2014.
- 1970
- Han, J., Zhao, Y., Wang, J., Zhang, B., Zhu, Y., Jiang, S., & Wang, L.: Effects of different land use types on potential evapotranspiration in the Beijing-Tianjin-Hebei region, North China. *Journal of Geographical Sciences*, 29(6), 922–934. doi:10.1007/s11442-019-1637-7, 2019.
- Helsel, D. R., R. M. Hirsch, K.R. Ryberg, S.A. Archfield, and E.J. Gilroy.: “Statistical Methods in Water Resources Techniques and Methods 4 – A3.” *USGS Techniques and Methods*, 2020.
- 1975
- 1980
- Hersbach, H., Bell, B., Berrisford, P., Hirahara, S., Horányi, A., Muñoz-Sabater, J., Nicolas, J., Peubey, C., Radu, R., Schepers, D., Simmons, A., Soci, C., Abdalla, S., Abellan, X., Balsamo, G., Bechtold, P., Biavati, G., Bidlot, J., Bonavita, M., De Chiara, G., Dahlgren, P., Dee, D., Diamantakis, M., Dragani, R., Flemming, J., Forbes, R., Fuentes, M., Geer, A., Haimberger, L., Healy, S., Hogan, R.J., Hólm, E., Janisková, M., Keeley, S., Laloyaux, P., Lopez, P., Lupu, C., Radnoti, G., de Rosnay, P., Rozum, I., Vamborg, F., Villaume, S., Thépaut, J-N.: Complete ERA5 from 1979: Fifth generation of ECMWF atmospheric reanalyses of the global climate. Copernicus Climate Change Service (C3S) Data Store (CDS). (Accessed on 06-06-2022), 2017.
- 1985
- 1990
- Hulsman, P., Hrachowitz, M., & Savenije, H. H. G.: Improving the Representation of Long-Term Storage Variations With Conceptual Hydrological Models in Data-Scarce Regions. *Water Resources Research*, 57(4). doi:10.1029/2020WR028837, 2021.
- 1995
- Hulsman, P., Winsemius, H. C., Michailovsky, C. I., Savenije, H. H. G., & Hrachowitz, M.: Using altimetry observations combined with GRACE to select parameter sets of a hydrological model in a data-scarce region. *Hydrology and Earth System Sciences*, 24(6), 3331–3359. doi:10.5194/hess-24-3331-2020, 2020.
- 2000
- Jeffers, J. N., & Boaler, S. B., 1966. Ecology of a miombo site. Lupa North Forest Reserve, Tanzania. I. Weather and plant growth , 1962–64’. *Ecology*, 54, 447–463.

- Jiménez, C., Prigent, C., Mueller, B., Seneviratne, S. I., McCabe, M. F., Wood, E. F., ... Wang, K.: Global intercomparison of 12 land surface heat flux estimates. *Journal of Geophysical Research Atmospheres*, 116(2), 1–27. doi:10.1029/2010JD014545, 2011.
- 2005 Jiménez, C., Prigent, C., & Aires, F.: Toward an estimation of global land surface heat fluxes from multisatellite observations. *Journal of Geophysical Research Atmospheres*, 114(6), 1–22. doi:10.1029/2008JD011392, 2009.
- Kleine, L., Tetzlaff, D., Smith, A., Dubbert, M., & Soulsby, C.: Modelling ecohydrological feedbacks in forest and grassland plots under a prolonged drought anomaly in Central Europe 2018–2020. *Hydrological Processes*, 35(8). doi:10.1002/hyp.14325, 2021.
- 2010 Kramer, K., Leinonen, I., & Loustau, D.: The importance of phenology for the evaluation of impact of climate change on growth of boreal, temperate and Mediterranean forests ecosystems: An overview. *International Journal of Biometeorology*. doi:10.1007/s004840000066, 2000.
- 2015 Leroux, L., Jolivot, A., Bégué, A., Lo Seen, D., and Zougrana, B.: “How Reliable Is the MODIS Land Cover Product for Crop Mapping Sub-Saharan Agricultural Landscapes?” *Remote Sensing* 6(9):8541–64. doi: 10.3390/rs6098541, 2014.
- Li, H., Ma, X., Lu, Y., Ren, R., Cui, B., & Si, B.: Growing deep roots has opposing impacts on the transpiration of apple trees planted in subhumid loess region. *Agricultural Water Management*, 258(June), 107207. doi: 10.1016/j.agwat.2021.107207, 2021.
- 2020 Liu, M., & Hu, D.: Response of Wetland Evapotranspiration to Land Use/Cover Change and Climate Change in Liaohe River Delta, China. *Water*; 11(5):955. <https://doi.org/10.3390/w11050955>, 2019.
- 2025 Liu, Wenbin, Lei Wang, Jing Zhou, Yanzhong Li, Fubao Sun, Guobin Fu, Xiuping Li, and Yan Fang Sang.: “A Worldwide Evaluation of Basin-Scale Evapotranspiration Estimates against the Water Balance Method.” *Journal of Hydrology* 538: 82–95. <https://doi.org/10.1016/j.jhydrol.2016.04.006>, 2016.
- 2030 Lu, P., Yu, Q., Liu, J., & Lee, X.: Advance of tree-flowering dates in response to urban climate change. *Agricultural and Forest Meteorology*, 138(1–4), 120–131. doi:10.1016/j.agrformet.2006.04.002, 2006.
- 2035 Macharia, D., Fankhauser, K., Selker, J. S., Neff, J. C., & Thomas, E. A.: Validation and Intercomparison of Satellite-Based Rainfall Products over Africa with TAHMO In Situ Rainfall Observations. *Journal of Hydrometeorology*, 23(7), 1131–1154. doi:10.1175/JHM-D-21-0161.1, 2022.
- Makapela, L.: *Review and use of earth observations and remote sensing in water resource management in South Africa : report to the Water Research Commission*, 2015.
- 2040 Marchesini, V. A., Fernández, R. J., Reynolds, J. F., Sobrino, J. A., & Di Bella, C. M.: Changes in evapotranspiration and phenology as consequences of shrub removal in dry forests of central Argentina. *Ecohydrology*, 8(7), 1304–1311. doi:10.1002/eco.1583, 2015.
- Martens, B., Miralles, D. G., Lievens, H., Van Der Schalie, R., De Jeu, R. A. M., Fernández-

- 2045 Prieto, D., ... Verhoest, N. E. C.: GLEAM v3: Satellite-based land evaporation and root-zone soil moisture. *Geoscientific Model Development*, 10(5), 1903–1925. doi:10.5194/gmd-10-1903-2017, 2017.
- Martins, J. P., Trigo, I., & Freitas, S. C. E.: Copernicus Global Land Operations "Vegetation and Energy" "CGLOPS-1". *Copernicus Global Land Operations*, 1–93. doi:10.5281/zenodo.3938963.PU, 2020.
- 2050 Miralles, D. G., Brutsaert, W., Dolman, A. J., & Gash, J. H.: On the Use of the Term "Evapotranspiration". *Water Resources Research*, 56(11). doi:10.1029/2020WR028055, 2020.
- Miralles, D. G., De Jeu, R. A. M., Gash, J. H., Holmes, T. R. H., & Dolman, A. J.: Magnitude and variability of land evaporation and its components at the global scale. *Hydrology and Earth System Sciences*, 15(3), 967–981. doi:10.5194/hess-15-967-2011, 2011.
- 2055 Mittermeier, R. A., Mittermeier, C. G., Brooks, T. M., Pilgrim, J. D., Konstant, W. R., Da Fonseca, G. A. B., & Kormos, C.: Wilderness and biodiversity conservation. *Proceedings of the National Academy of Sciences of the United States of America*, 100(18), 10309–10313. doi:10.1073/pnas.1732458100, 2003.
- 2060 Mu, Q., Zhao, M., and Running, W.S.: Improvements to a MODIS Global Terrestrial Evapotranspiration Algorithm. *Remote Sensing of Environment* 115 (8): 1781–1800. <https://doi.org/10.1016/j.rse.2011.02.019>, 2011.
- 2065 Mu, Q., Heinsch, F. A., Zhao, M., & Running, S. W.: Development of a global evapotranspiration algorithm based on MODIS and global meteorology data. *Remote Sensing of Environment*, 111(4), 519–536. doi:10.1016/j.rse.2007.04.015, 2007.
- 2070 Myneni, R., Knyazikhin, Y., and Park, T.: MCD15A2H MODIS/TerraAqua Leaf Area Index/FPAR 8-day L4 Global 500m SIN Grid V06, NASA EOSDIS Land Processes DAAC [data set], <https://doi.org/10.5067/MODIS/MCD15A2H.061>, 2021.
- Myneni, R., & Park, Y. K.: *MCD15A2H MODIS/Terra+Aqua Leaf Area Index/FPAR 8-day L4 Global 500m SIN Grid V006*. NASA EOSDIS Land Processes DAAC. Retrieved from <https://doi.org/10.5067/MODIS/MCD15A2H.006>, (last accessed: 20 January, 2023) 2015.
- 2075 [Nelson, Michael, Tim Hill, William Remus, and Marcus O'connor. "Time Series Forecasting Using Neural Networks: Should the Data Be Deseasonalized First?" *Journal of Forecasting* 18: 359–67, 1999.](#)
- 2080 Niu, S., Fu, Y., Gu, L., and Luo, Y.: Temperature Sensitivity of Canopy Photosynthesis Phenology in Northern Ecosystems. Pp. 503–19 in *Phenology: An Integrative Environmental Science*, edited by M. D. Schwartz., 2013.
- Nord, E. A., & Lynch, J. P.: Plant phenology: A critical controller of soil resource acquisition. *Journal of Experimental Botany*, 60(7), 1927–1937. doi:10.1093/jxb/erp018, 2009.

- 2085 Novick, K. A., Ficklin, D. L., Stoy, P. C., Williams, C. A., Bohrer, G., Oishi, A. C., Papuga, S. A.,
Blanken, P. D., Noormets, A., Sulman, B. N., Scott, R. L., Wang, L., & Phillips, R. P.: The
increasing importance of atmospheric demand for ecosystem water and carbon fluxes.
Nature Climate Change, 6(11), 1023–1027. doi:10.1038/nclimate3114, 2016.
- 2090 ORNL DAAC., 2018. MODIS and VIIRS Land Products Global Subsetting and
Visualization Tool, Subset obtained for MCD12Q2 product at [-12:76252], [32.48406],
time period: [31-12-2020] to [31-12-2021], and subset size: [4]_[4] km, ORNL DAAC,
Oak Ridge, Tennessee, USA [data set], <https://doi.org/10.3334/ORNLDAAC/1379>.
- 2095 Pelletier, J., Paquette, A., Mbindo, K., Zimba, N., Siampale, A., Chendauka, B., Siangulube, F.,
& Roberts, J. W.: Carbon sink despite large deforestation in African tropical dry forests
(miombo woodlands). *Environmental Research Letters*, 13(9). doi:10.1088/1748-
9326/aadc9a, 2018.
- 2100 Pereira, C. C., Boaventura, M. G., Cornelissen, T., Nunes, Y. R. F., & de Castro, G. C.: What
triggers phenological events in plants under seasonal environments? A study with
phylogenetically related plant species in sympatry. *Brazilian Journal of Biology*,
84(March). doi:10.1590/1519-6984.257969, 2022.
- Roberts, J. M.: *The role of forests in the hydrological cycle. Forests and forest plants* (Vol. III).
Retrieved from <https://www.eolss.net/sample-chapters/c10/E5-03-04-02.pdf>, last accessed:
20 June, 2022, (not dated).
- 2105 Running, Steven W, Qiaozhen Mu, Maosheng Zhao, A. M.: User 's Guide MODIS Global
Terrestrial Evapotranspiration (ET) Product NASA Earth Observing System MODIS Land
Algorithm (For Collection 6) (last accessed: 20 January, 2023), 2019.
- 2110 Ryan, C. M., Pritchard, R., McNicol, I., Owen, M., Fisher, J. A., & Lehmann, C.: Ecosystem
services from southern African woodlands and their future under global change.
Philosophical Transactions of the Royal Society B: Biological Sciences, 371(1703).
doi:10.1098/rstb.2015.0312, 2016.
- Saha, S., Moorthi, S., Wu, X., Wang, J., & Coauthors.: The NCEP Climate Forecast System
Version 2. *Journal of Climate*, 27, 2185–2208. doi:10.1175/JCLI-D-12-00823.1, 2014.
- 2115 Saha, S., Moorthi, S., Pan, H., Wu, X., Wang, J., & Coauthors.: The NCEP Climate Forecast
System Reanalysis. *Bulletin of the American Meteorological Society*, 91, 1015–1057.
doi:10.1175/2010BAMS3001.1, 2010.
- 2120 Santin-Janin, H., Garel, M., Chapuis, J. L., & Pontier, D.: Assessing the performance of NDVI as
a proxy for plant biomass using non-linear models: A case study on the kerguelen
archipelago. *Polar Biology*, 32(6), 861–871. doi:10.1007/s00300-009-0586-5, 2009.
- Savenije, H. H.G.: HESS opinions ‘topography driven conceptual modelling (FLEX-Topo)’.
Hydrology and Earth System Sciences, 14(12), 2681–2692. doi:10.5194/hess-14-2681-2010,
2010.

- 2125 Savenije, Hubert H.G.: The importance of interception and why we should delete the term evapotranspiration from our vocabulary. *Hydrological Processes*, 18(8), 1507–1511. doi:10.1002/hyp.5563, 2004.
- Savory, B. M.: Site quality and tree root morphology in Northern Rhodesia, Rhodes. *J. Agricult. Res.*, 1, 55–64, 1963.
- 2130 Schwartz, M. D.: *Phenology: An Integrative Environmental Science*. (M. D. Schwartz, Ed.), *Phenology: An Integrative Environmental Science* (Second Edi). Dordrecht: Springer Netherlands. doi:10.1007/978-94-007-6925-0_27, 2013.
- 2135 Senay, G. B., Bohms, S., Singh, R. K., Gowda, P. H., Velpuri, N. M., Alemu, H., & Verdin, J. P.: Operational Evapotranspiration Mapping Using Remote Sensing and Weather Datasets: A New Parameterization for the SSEB Approach. *Journal of the American Water Resources Association*, 49(3), 577–591. doi:10.1111/jawr.12057, 2013.
- Shahidan, M. F., Salleh, E., & Mustafa, K. M. S.: Effects of tree canopies on solar radiation filtration in a tropical microclimatic environment. *Sun, Wind and Architecture - The Proceedings of the 24th International Conference on Passive and Low Energy Architecture, PLEA 2007*, (November), 400–406, 2007.
- 2140 Sheil, D.: Forests, atmospheric water and an uncertain future: the new biology of the global water cycle. *Forest Ecosystems*, 5(1). doi:10.1186/s40663-018-0138-y, 2018.
- Snyder, R. L., & Spano, D.: Phenology and Evapotranspiration. In Mark D. Schwartz (Ed.), *Phenology: An Integrative Environmental Science* (Second, pp. 521–528). Milwaukee, 2013.
- 2145 Stancalie, G., & Nert, A.: Possibilities of Deriving Crop Evapotranspiration from Satellite Data with the Integration with Other Sources of Information. *Evapotranspiration - Remote Sensing and Modeling*, (January). doi:10.5772/23635, 2012.
- 2150 Stöckli, R., T. Rutishauser, I. Baker, M. A. Liniger, and A. S. Denning.: “A Global Reanalysis of Vegetation Phenology.” *Journal of Geophysical Research: Biogeosciences* 116 (3): 1–19. <https://doi.org/10.1029/2010JG001545>, 2011.
- Tian, F., Wigneron, J. P., Ciais, P., Chave, J., Ogée, J., Peñuelas, J., ... Fensholt, R.: Coupling of ecosystem-scale plant water storage and leaf phenology observed by satellite. *Nature Ecology and Evolution*, 2(9), 1428–1435. doi:10.1038/s41559-018-0630-3, 2018.
- 2155 Tuzet, A. J.: Stomatal Conductance, Photosynthesis, and Transpiration, Modeling. In J. Gliński, J., Horabik, J., Lipiec (Ed.), *Encyclopedia of Agrophysics. Encyclopedia of Earth Sciences Series* (pp. 855–858). Dordrecht. doi:10.1007/978-90-481-3585-1_213, 2011.
- 2160 Urban, J., Ingwers, M. W., McGuire, M. A., & Teskey, R. O.: Increase in leaf temperature opens stomata and decouples net photosynthesis from stomatal conductance in *Pinus taeda* and *Populus deltoides* x *nigra*. *Journal of Experimental Botany*, 68(7), 1757–1767. doi:10.1093/jxb/erx052, 2017.
- Van Der Ent, R. J., Wang-Erlandsson, L., Keys, P. W., & Savenije, H. H. G.: Contrasting roles

- of interception and transpiration in the hydrological cycle – Part 2: Moisture recycling. *Earth System Dynamics*, 5(2), 471–489. doi:10.5194/esd-5-471-2014, 2014.
- 2165 Van Der Ent, Rudi J., Savenije, H. H. G., Schaefli, B., & Steele-Dunne, S. C.: Origin and fate of atmospheric moisture over continents. *Water Resources Research*, 46(9), 1–12. doi:10.1029/2010WR009127, 2010
- Vermote, E., Wolfe, R.: MOD09GA MODIS/Terra Surface Reflectance Daily L2G Global 1km and 500m SIN Grid V006 [Data set]. NASA EOSDIS Land Processes DAAC. Accessed 2022-10-01 from <https://doi.org/10.5067/MODIS/MOD09GA.006>, 2015.
- 2170 Vinya, R., Malhi, Y., Brown, N. D., Fisher, J. B., Brodribb, T., & Aragão, L. E.: Seasonal changes in plant–water relations influence trends of leaf display in Miombo woodlands: evidence of water conservative strategies. *Tree Physiology*, 39, 04–112. doi:doi:10.1093/treephys/tpy062, 2018.
- 2175 Wang, S., Fu, B. J., Gao, G. Y., Yao, X. L., & Zhou, J.: Soil moisture and evapotranspiration of different land cover types in the Loess Plateau, China. *Hydrology and Earth System Sciences*, 16(8), 2883–2892. doi: 10.5194/hess-16-2883-2012, 2012.
- Wang-Erlandsson, L., Bastiaanssen, W. G. M., Gao, H., Jägermeyr, J., Senay, G. B., Van Dijk, A. I. J. M., ... Savenije, H. H. G.: Global root zone storage capacity from satellite-based evaporation. *Hydrology and Earth System Sciences*, 20(4), 1459–1481. doi:10.5194/hess-20-1459-2016, 2016.
- 2180 WARMA.: Catchments for Zambia. Retrieved 9 February 2022, from <http://www.warma.org.zm/catchments-zambia/luangwa-catchment-2/>, 2022.
- 2185 Weerasinghe, I., Bastiaanssen, W., Mul, M., Jia, L., & Van Griensven, A.: Can we trust remote sensing evapotranspiration products over Africa. *Hydrology and Earth System Sciences*, 24(3), 1565–1586. doi:10.5194/hess-24-1565-2020, 2020.
- Wehr, R., Commane, R., Munger, J. W., Barry Mcmanus, J., Nelson, D. D., Zahniser, M. S., ... Wofsy, S. C.: Dynamics of canopy stomatal conductance, transpiration, and evaporation in a temperate deciduous forest, validated by carbonyl sulfide uptake. *Biogeosciences*, 14(2), 389–401. doi:10.5194/bg-14-389-2017, 2017.
- 2190 White, F.: *The Vegetation of Africa; a descriptive memoir to accompany the UNESCO/AETFAT/UNSO vegetation map of Africa*. Paris: UNESCO. Retrieved from <https://unesdoc.unesco.org/ark:/48223/pf0000058054> (Last accessed: 20 January, 2023), 1983.
- 2195 World Bank.: "The Zambezi River Basin: A Multi-Sector Investment Opportunities Analysis – State of the Basin," World Bank Publications - Reports 2961, The World Bank Group. <https://ideas.repec.org/p/wbk/wboper/2961.html>. (Last accessed: 20 January 2023), 2010.
- 2200 Zhang, K, Kimball, S. J., and Running, W.S.: A Review of Remote Sensing Based Actual Evapotranspiration Estimation. *Wiley Interdisciplinary Reviews: Water* 3 (6): 834–53. <https://doi.org/10.1002/wat2.1168>, 2016.

- 2205 Zhang, X., Friedl, M. A., Schaaf, C. B., Strahler, A. H., Hodges, J. C. F., Gao, F., Reed, B. C., &
Huete, A.: Monitoring vegetation phenology using MODIS. *Remote Sensing of Environment*, 84(3), 471–475. doi: 10.1016/S0034-4257(02)00135-9, 2003.
- Zhao, M, Peng, C., Xiang, W., Deng, X., Tian, D., Zhou, X., Yu, G., He, H., and Zhao, Z.: “Plant Phenological Modeling and Its Application in Global Climate Change Research: Overview and Future Challenges.” *Environmental Reviews* 21 (1): 1–14. <https://doi.org/10.1139/er-2012-0036>, 2013
- 2210 Zimba, H., Coenders-Gerrits, M., Banda, K., Schilperoort, B., van de Giesen, N., Nyambe, I., and Savenije, H. H. G.: Phenophase-based comparison of field observations to satellite-based actual evaporation estimates of a natural woodland: miombo woodland, southern Africa, *Hydrol. Earth Syst. Sci.*, 27, 1695–1722, <https://doi.org/10.5194/hess-27-1695-2023>, 2023.
- 2215
- Zimba, H., Coenders, M., Savenije, H. H. G., van de Giesen, N., & Hulsman, P.: ZAMSECUR Project Field Data Mpika, Zambia (Version 2) [Data set]. 4TU.ResearchData. <https://doi.org/10.4121/19372352.V2>, 2022.
- 2220